Journal of Materials Chemistry A

ROYAL SOCIETY OF CHEMISTRY

PERSPECTIVE

View Article Online
View Journal | View Issue

Cite this: J. Mater. Chem. A, 2023, 11, 17452

Progressing thin-film membrane designs for post-combustion CO_2 capture: performance or practicality?

Ji Wu, Febrian Hillman, Can-Zeng Liang, Yuewen Jia and Sui Zhang *

Tremendous potential is seen in membrane technology for realizing efficient post-combustion CO_2 capture from power plant flue gas, the largest anthropogenic source of emission. However, an examination of existing literature revealed a substantial gap between the sheer number of lab-scale materials with extraordinary CO_2/N_2 separation performance and the small fragment of large-scale commercial developments that still perform below the new competitive industrial targets. An effective material approach aiming to bridge this gap is the multilayer thin-film composite (TFC) membrane design, which allows for the transformation of thick dense membranes with excellent theoretical intrinsic performances into a practical thin (<1 μm) to ultrathin-film (<100 nm) configuration with high CO_2 permeance and CO_2/N_2 selectivity. Unavoidably, many design constraints surfaced during this transition due to the challenges of ultrathin-film fabrication, porous substrate design, increased vulnerability and deviation of gas transport properties at the thin-film state, which all compromise the scalability of TFC membranes. Yet, these constraints are often overlooked topics in current TFC membrane studies as they are generally performance-pursuing and tend to be more zealous about the discovery or re-innovating of novel selective layer materials with less concern over practicality issues. In this perspective, key existing TFC design criteria are revisited for each TFC component/layer with a critical evaluation of their oversight for some of the practical considerations, while keen research suggestions are being made in areas that could potentially enhance the performance or scalability of current designs, such as materials recommendation, structural modification targets, mechanistic study of thin-film state transport, and knowledge development for upscaling. Besides the conventional layer-on-layer TFC design, an integrated layer concept established on a microporous gutter layer is also proposed here. Lastly, the potential for translating existing flat sheet TFC designs into the industrially favorable hollow fiber configuration has been quite rigorously assessed.

Received 13th May 2023
Accepted 17th July 2023

DOI: 10.1039/d3ta02842a

rsc.li/materials-a

1. Introduction

The Earth's climate is currently struggling with a record-high anthropogenic CO_2 emission of over 36 billion tons every year from energy generation, with about 65% being contributed by the combustion of coal and gas in power plants.[1,2] Tremendous research efforts especially since the 2010s have been devoted to the development of effective CO_2 capture technologies targeting the massive post-combustion flue gas streams discharged from power plants.[3,4] The flue gas composition varies from plant to plant, but in general its CO_2 concentration ranges from 11 to 14% for coal-fired plants and 4% to 8% for gas-fired ones, balanced with primarily N_2, some O_2 and water, and minor quantities of contaminants like SO_x and NO_x.[5,6] Therefore, the key molecular partitioning occurring during post-combustion CO_2 capture is essentially the separation of CO_2 gas molecules from N_2 (*i.e.* CO_2/N_2 separation). The basic requirements for such separations in practical applications include not only energy- and cost-efficiency, but also sufficient recovery (>90%) and purity (>95%) to be industrially meaningful.[7] The current leading technology is still the traditional amine absorption process which is energy-intensive due to the high thermal input required for the release of CO_2 from the amine solutions at elevated temperatures.[8] About 30% of total energy output will be expended to achieve satisfactory CO_2 removal by amine absorption, rendering it an economically unsustainable technology for post-combustion CO_2 capture.[7] Clearly, there is a pressing need for a disruptive alternative technology that could circumvent this conventional pitfall.

Gas separation membranes have received extensive research attention over the past decade for their distinct advantages over absorption as an emerging post-combustion CO_2 capture technology. The CO_2/N_2 separation *via* membranes requires no thermal input or solvent regeneration, offering a much more energy-efficient process with about 90% saving on the heating

Department of Chemical and Biomolecular Engineering, National University of Singapore, Singapore 117585, Singapore. E-mail: chezhangsui@nus.edu.sg

cost.[9] It also operates with a smaller footprint *via* modular designs and runs continuously. Tremendous efforts have been made in the academy and industry over the past decades for membrane-based post-combustion carbon capture.

2. Membrane-based post-combustion CO_2 capture

2.1. Transport mechanism of membrane-based CO_2/N_2 separation

For gas separation, polymers are the most prevalent membrane materials from research to commercial implementation owing to their extraordinary film-forming ability and large-scale processability. They are generally fabricated as thin, dense films that selectively permeate gas molecules under a trans-membrane pressure *via* the well-adopted solution–diffusion mechanism as illustrated in Fig. 1.[10] That is, the gas penetrants first adsorb onto the membrane surface and then diffuse through thermally agitated transient gaps between densely packed but mobile polymer chains, followed by eventually desorbing away from the permeate side. Therefore, gas solubility (S, associated with gas condensability and sorption in the membrane) and diffusivity (D, associated with gas kinetic diameter and diffusion through the membrane) are two critical transport parameters that determine the overall permeability (P) and selectivity (α) of a dense polymeric membrane for a particular gas species.[10] More specifically, the solution–diffusion mechanism expresses the permeability of dense polymers as the product of their diffusivity and solubility coefficients ($P = D \times S$), and selectivity for one gas over the other is simply a ratio between their respective permeabilities ($\alpha = P_i/P_j$).

Polymeric membranes have found commercial applications for separating a number of gas pairs, such as O_2/N_2 (air separation), H_2/N_2 or CH_4 (hydrogen purification) and CO_2/CH_4 (natural gas processing).[11–14] The discrimination of these gas molecules is largely dependent on size sieving, and thus glassy polymers with relatively more rigid polymer chains that manifest a high diffusivity selectivity are usually used.[15] However, in CO_2/N_2 separation, although CO_2 has a smaller kinetic diameter than N_2 (3.3 Å *vs.* 3.64 Å), its critical volume is larger than that of N_2 (93.9 *vs.* 89.8 $cm^3\ mol^{-1}$) so that their diffusivity selectivity in polymeric membranes is generally very low and not an effective transport factor to explore as compared with gas pairs with clearly differentiated molecular sizes.[16–18] In contrast, the high condensability of CO_2 makes membrane materials with solubility-governed preferential permeation of CO_2 over N_2 a much more favorable option.[7] In this sense, rubbery polymers with mobile polymer backbones and high CO_2/N_2 solubility selectivity, like polydimethylsiloxane (PDMS) and polyethylene oxide (PEO) based polymers, or glassy polymers with large free volume as extra CO_2 sorption sites, such as polymers of intrinsic microporosity (PIMs), polyacetylenes (*e.g.* poly(1-trimethylsilyl-1-propyne) (PTMSP)) and fluoropolymers (*e.g.* AF2400), are the ideal CO_2/N_2 separation membrane materials.[19–23]

In addition to polymers, other materials have also been repeatedly reported for post-combustion CO_2 capture, such as two-dimensional (2D) materials, framework materials and zeolites.[9,20] Instead of solution–diffusion, gas molecules permeate through these materials *via* surface diffusion where surface adsorption plays an important role, molecular sieving or other mechanisms.

2.2. Limitations of current membranes for CO_2/N_2 separation

The current membranes for CO_2/N_2 separation are challenged by a few limitations. First is the well-known performance trade-off characteristic of polymers whereby a high permeability generally comes with a low selectivity and *vice versa* due to the insufficient chain rigidity or lack of strong polymer–penetrant interaction according to the transient state theory.[23,24] This trade-off behavior, empirically illustrated by a log–log relationship between the permeability and selectivity known as the

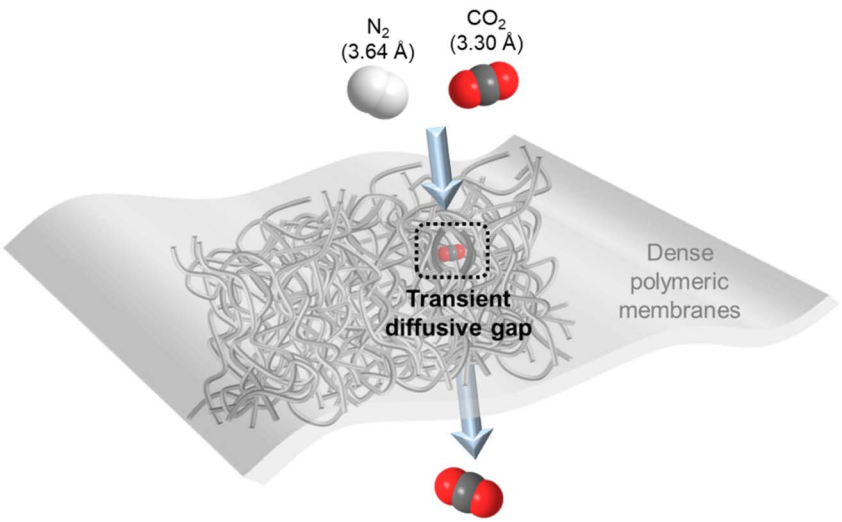

Fig. 1 Illustration of CO_2/N_2 separation through a dense polymeric membrane.

Robeson upper bound (Fig. 2a), puts a limit on the separation efficiency achievable by a given polymer material. When dealing with the massive volume of flue gas which is several times larger than most other industrial gas separations, the most permeable types of polymers are desired but their selectivity would typically be too low for the separation unit to meet the product purity requirement.[7]

Another tricky issue with separating highly condensable species is their plasticization effect on both glassy and rubbery polymers. Plasticization occurs when the solvation effect of condensable gases under high pressures, like CO_2, leads to the irreversible intercalation of penetrants between polymer chains that disrupts the chain packing, increases chain mobility and enhances the permeance of non-plasticizing N_2 more than proportionally, eventually causing a catastrophic loss of selectivity.[14,24] Even though flue gas usually has a low pressure of around 1–2 bar (CO_2 partial pressure is even lower) which is not a plasticization-inducing pressure range, the solvation effect of CO_2 after long-term exposure could still be considerable.[9] A performance test with a sufficiently long duration is necessary to assess the membrane stability against plasticization for CO_2/N_2 separation. For high-free volume glassy polymers, physical aging is the most infamous problem associated with their membrane design, which causes their gas permeability to decrease significantly with time due to the gradual relaxation and subsequent collapse of the thermodynamically unstable, non-equilibrium excess free volume in the polymers.[25,26]

Third, to reach high efficiency, practical membranes require fast gas permeation, represented by the permeance (pressure-normalized flux) of membranes which is given by the equation: permeance (in gas permeation units, GPU) = permeability (in Barrer)/thickness (in μm). Processing membrane materials into a supported thin film is a major challenge met in the upscaling of membrane technologies. Details will be discussed in Section 3.

Right now, only a few commercial polymeric CO_2/N_2 membranes, including Polyactive®, Polaris™, polyvinylamine (PVAm) and polyether ether ketone (PEEK) have been verified at or beyond a pilot scale (technology readiness level (TRL) 6) with separation performances near or beyond the earliest established industrial targets (CO_2 permeance >1000 GPU and optimal CO_2/N_2 selectivity ~20–60).[7,27–31] PRISM™ membranes are also commercial products verified at a pilot-scale but their separation performances are way below the bar.[32] Among them, only the Gen 1 Polaris™ membranes have recently reached the demonstration scale (TRL 7–8), which are by far the largest practical post-combustion CO_2 capture system ever developed.[33] While hundreds or even thousands of membrane materials with excellent intrinsic CO_2/N_2 performance have been created in the labs as thick dense films over the past decade, there appears to be a distinct gap between the "promising" materials available in the literature and practical membranes in use. To address this gap, the concept of membrane configuration (*i.e.* optimizing the membrane dimensions, geometry and assembly) has started to receive increasing research attention because it is one of the keys to endowing these lab materials with a practically working form.

3. From thick dense films to practical thin-skinned membranes

3.1. Impracticality in thick dense films

Discovering and re-innovating membrane materials with intrinsic performance surpassing the Robeson upper bound forms a huge portion of the entire membrane post-combustion CO_2 capture research, especially after the establishment of the CO_2/N_2 upper bound in 2008.[34] Interestingly, the concept of upper bound was proposed as early as in 1991 for quite a number of industrially important gas separations without the inclusion of CO_2/N_2 because no practical interest was

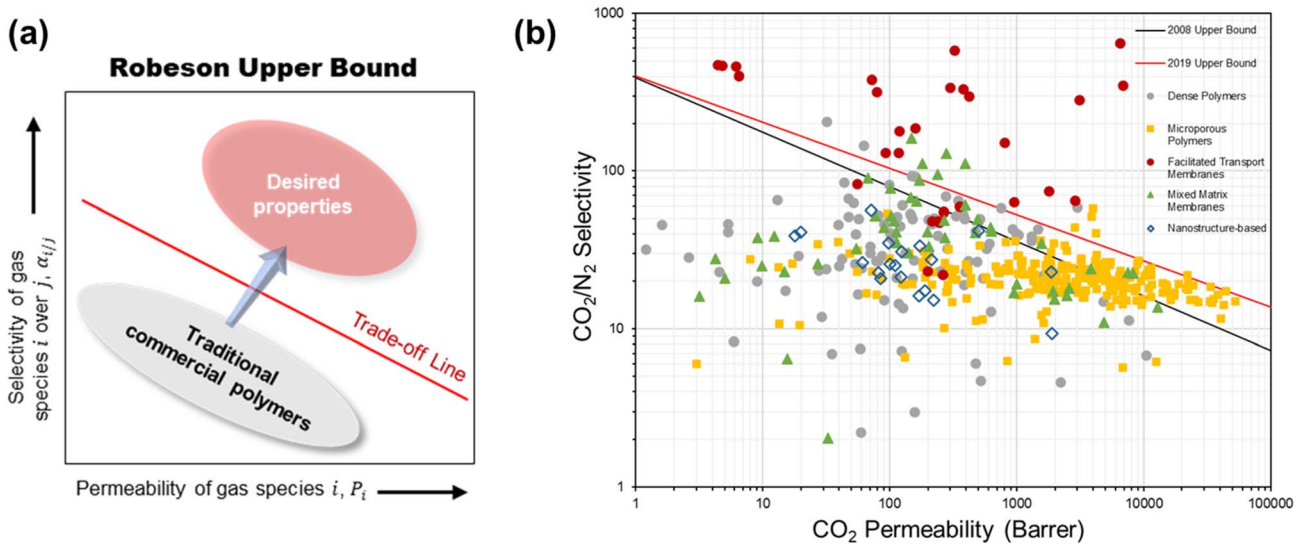

Fig. 2 (a) A simplified Robeson upper bound plot. (b) Summary of the intrinsic CO_2/N_2 separation performance of existing representative materials against the 2008 and 2019 upper bounds.

considered for this separation at that time.[21,35] The existing CO_2/N_2 membrane studies covered a wide spectrum of materials, which initially fell largely within the realm of organic polymers but soon expanded into other classes of molecular architectures or their polymer-hosted hybrids since the advent of framework structures. Interesting to note here is that although the upper bound was originally developed upon dense polymers based on the solution–diffusion transport mechanism, it became a prevailing standard for benchmarking the intrinsic performance of many new materials that separated gas molecules *via* different mechanisms (*e.g.* surface diffusion, molecular sieving, or reversible reactions).

For polymers, the representative materials advancement ranges from chemical modification, functionalization or copolymerization of traditional rubbery polymers, such as PEO or PDMS, with more CO_2-philic components for the synthesis of more rigid and contorted microporous glassy polymers with ever higher fractional free volume (FFV) and CO_2 solubility, including the early PIM, PIM-PI structures and new ultrapermeable 2D PIMs.[9,21,36] The extraordinary intrinsic performance of the new PIM structures even promoted the revision of the CO_2/N_2 upper bound for polymeric membranes in 2019.[21] On the other hand, a huge variety of non-polymer-based materials, including inorganics like zeolites and silicas, framework structures like metal organic frameworks (MOFs) and covalent organic frameworks (COFs), 2D nanosheets like graphene and graphene oxides (GO), CO_2-reactive additives like amino acid salts and ionic liquids (ILs), and many more, have also been explored for membrane CO_2/N_2 separation.[18,37–44] Given their limited ability to form free-standing films, these materials are usually fabricated as supported membranes or physically blended with polymers to form hybrid nanocomposite membranes, which are also known as mixed matrix membranes (MMM).[9,25,45]

As shown by the performance summary in Fig. 2b, quite a number of these state-of-the-art membranes demonstrated outstanding intrinsic CO_2/N_2 separation performance near or above the latest 2019 trade-off limit, which seems to give a very promising outlook for membrane post-combustion CO_2 capture. However, the majority of these intrinsic-performance investigations on new materials, especially for polymers and polymer-based MMMs, were conducted using thick dense films of several to several tens of micrometers. Such membrane configuration is undeniably impractical for real application because the gas flux through this kind of thick, barrier materials is too slow from a process point of view, even if they possess very high intrinsic permeabilities. However, for nanostructure-based membranes, many of which were fabricated and studied as thin films (on a support), they suffer from an extremely low scalability as compared with polymer-based materials at this stage.[37,39,41]

3.2. Importance of thin-film membrane development

In the context of CO_2 capture from the large volume of flue gases, the membrane system is to be designed with high CO_2 permeance to meet the enormous process throughput requirement, which can hardly be achieved by any thick symmetric dense membrane. Most importantly, the low partial pressure of CO_2 in the flue gas feed renders the CO_2/N_2 separation a pressure-ratio limited process such that enhancing the gas permeance is more meaningful and cost-saving than raising the selectivity. A minimum CO_2 permeance of 1000 GPU is typically required as revealed by simulation studies to make the process economically viable, and it is always preferred to have a membrane with higher permeance as it offers higher throughput and smaller area requirement.[7]

While both increasing the intrinsic permeability and reducing the thickness of the membrane could enhance the permeance, almost none of the current materials in their thick dense film form can afford sufficient permeance for CO_2/N_2 separation. Processing them into thin-skinned membranes is desired. Substantial research efforts have recently been channeled to the design of thin-film (<1 μm) or ultrathin-film (<100 nm) membranes with industrially practical levels of CO_2 permeance (at least >1000 GPU) using polymers with high intrinsic CO_2/N_2 separation performance, including but not limited to PDMS, PEO-based polymers, PVAm and PIMs.[9,18,46–49] This presents a significant advancement of membranes for post-combustion CO_2 capture towards a more practicality-driven stage, though further development is still needed. In the meantime, research to break the intrinsic performance ceiling is still of profound value to this field because there are processable limits to thickness reduction, beyond which only higher intrinsic permeability could more effectively bring about higher permeance.

Meanwhile, studies suggested a moderate CO_2/N_2 selectivity of >20 is already sufficient for handling the dilute feed involved in post-combustion CO_2 capture, and further increases would drastically drive up the membrane area requirement with only marginal improvement in the permeate purity due to a pressure-ratio limitation of 5–10 in practical applications to keep the compression cost in check.[7,50] Based on these criteria, most TFC studies agreed on an empirical range of industrial targets of a CO_2 permeance of >1000 GPU or as high as possible and an optimal CO_2/N_2 selectivity of ~20–60 with the higher end being a relatively looser number depending on the available pressure ratio. After over a decade of development, new competitive CO_2 permeance targets of >3000 GPU have also been proposed which makes perfect sense given the rate of flue gas emission.[18] Nevertheless, this does not mean that a highly CO_2/N_2 selective membrane is not useful. From a process design perspective, simulation studies revealed that it is too difficult and costly for a membrane separation unit, no matter how permeable and selective, to deliver the desired recovery and purity simultaneously with just one stage given a dilute CO_2 feed.[7] Therefore, a number of studies agreed that the design of a two-stage membrane separation unit would be more favorable for post-combustion CO_2 capture, with the first stage using high-permeance, modestly selective membranes to concentrate the CO_2 at high recovery, followed by a second stage using highly selective membranes to further purify the permeate without the pressure-ratio limitation.[7,9,50,51] Still, for the second stage, an optimal selectivity range exists, which depends on the available

CO_2 concentration and the CO_2 permeance, due to the need to balance the membrane area requirement.[50] Fabrication of membranes with sufficient selectivity relies on both the intrinsic material property and thin film processing techniques to minimize defects.

4. Fundamentals of thin-film composite (TFC) membranes

Thin-skinned membranes, featuring at least a thin skin layer for fast selective permeation and a thick support layer for mechanical support, usually exist in two different forms: integral asymmetric membranes and TFC membranes. For CO_2/N_2 separation, TFC design is the mainstream and will be discussed in detail in this section.

4.1. Layer-on-layer TFC design and the functions of each layer

The most established thin-film membrane configuration is the multilayer thin-film composite (TFC) structure (Fig. 3a) in which a thin selective layer made of dense polymers or other CO_2/N_2-selective materials is deposited, typically *via* a solution-coating technique, on a porous substrate with an optional interlayer, called the gutter layer, in between them. Fig. 3b and c illustrate the structures of a common two-layer and three-layer TFC membrane design. In some cases, an additional fourth

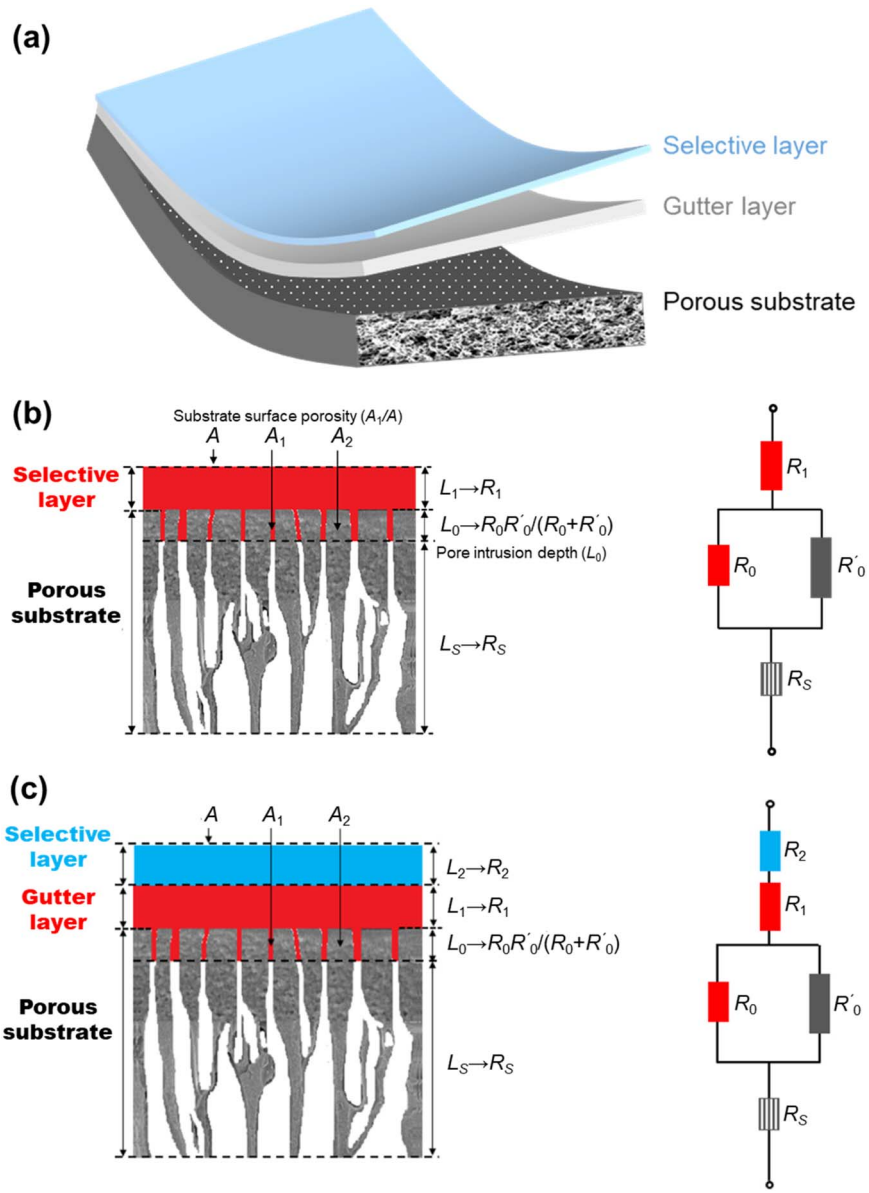

Fig. 3 (a) Illustration of the multilayered structure of thin-film composite (TFC) membranes; schematics demonstrating the analogous resistance model interpretations of (b) two-layer and (c) three-layer TFC membrane structures, respectively (reproduced with permission,[24] copyright 2019, Elsevier Ltd).

thin protective layer is applied on top to seal nanoscale pinholes and maintain the integrity of the delicate selective layer.[9] Such a thin selective layer structure not only boosts the permeance, but also reduces the membrane cost, as it consumes only little selective material (usually the most expensive component) while the support and gutter layers could be made of cheap commercial materials.[24] On top of that, TFC is also an extremely versatile and expandable design platform in the sense that any selective material coatable as a film, even the exotic or expensive ones, could potentially be used to form the selective layer, which has led to much non-polymer-based TFC membrane research.[52]

Within a TFC design, each layer has its own functions and design criteria but they are also mutually influenced by other layers at the same time. The purpose of the porous substrates is mainly to provide the mechanical support for the selective layer because at the ultra-thin state no free-standing films could withstand the rigor of large-scale processing. Its porous nature, on the other hand, is to ensure minimal gas transport resistance from the support and hence high overall gas permeance in the resulting TFC membrane. Asymmetric polymeric substrates with a porous skin layer made from commercial polymers, such as polyacrylonitrile (PAN), polysulfone (PSF) and polyethersulfone (PES), are the most commonly used substrate materials in TFC owing to their low cost, ease of processing and mechanical flexibility.[53–56]

The function of the gutter layer is to prevent the penetration of selective layer materials into the surface pores of the substrate, which will otherwise drastically increase the gas transport resistance at the skin layer because the selective material coating solution is typically made very dilute with low viscosity to obtain the desired ultra-thinness. Also, it serves as a protective interlayer that keeps the polymeric substrates from directly contacting the destructive aprotic organic solvents used by a number of selective polymer materials. PDMS is by far the most prevalent gutter layer material used in TFC studies because of its high CO_2 permeability to minimize transport resistance, low surface energy for easy adhesion, ease of processing, good solvent stability, resistance against plasticization and common contaminants, commercial availability and low cost.[19,57–60] Solution coating is a common technique for depositing the gutter layer.

For the selective layer, it is essentially a dense membrane reduced to a surface-confined ultra-thin configuration that separates gas molecules through the same inherent gas transport mechanism. The selective layer in most cases contributes the majority of transport resistance and gas-discrimination ability in a TFC membrane so that materials with high permeability, sufficient selectivity and ultra-thin film-forming ability are most desired.

4.2. Series resistance model for assessing TFC separation performance

The compounded gas separation properties of the TFC are usually analyzed by a series resistance model which analogizes the permeation of gas through the layer-on-layer component arrangement of TFC to the electrical current flowing through multiple resistors in series, depicted by Fig. 3c and d.[24,61] For a two-layer design with inevitable intrusion of the selective layer solution into the substrate pores, several assumptions need to be made for the model to work quantitatively, including a one-dimensional gas diffusion pathway, equidistant intrusion depth, and pressure-and-thickness-independence of selective layer permeability.[61] Modified and improved models have also been proposed by a number of studies.[62–64] For a three-layer design that includes a dense smooth gutter layer, quantitative analysis will be easier because there is no intrusion of the selective layer into the gutter layer. Therefore, by considering the gutter-coated substrate as one resistance-contributing block, the gas permeance of a three-layer TFC membrane, J_C (in GPU), can be simply estimated according to this equation derived from the resistance model:

$$1/J_C = l_S/P_S + 1/J_B \quad (1)$$

where P_S and l_S are the intrinsic permeability (in Barrer) and thickness of the selective layer, respectively, and J_B is the gas permeance (in GPU) of the porous substrate with gutter layer coating.[24,52] Nevertheless, to investigate the individual effect of the gutter layer on the overall performance, assumptions on the intrusion depth are still necessary.[65] Also, for emerging nanostructure-based gutter layer materials, such as MOFs, that tend to form crystal-like, irregular interfaces with the selective layer, estimation of the average thickness of the selective layer could be an issue in conducting accurate modelling analyses.

4.3. Difference from integrally skinned composite membranes

In fact, the concept of anisotropic composite membrane dates back to early commercial gas separation applications (*e.g.* air separation and hydrogen purification) where PDMS-coated integrally skinned asymmetric (IAS) polymeric membranes fabricated from non-solvent induced phase separation (NIPS) with defect-free skin layers acting as the selective layer have been often used (*i.e.* the Loeb–Sourirajan type asymmetric membranes).[66–69] However, the raw material requirement for such a design is enormous (~25–50 times more than TFC) as both the bulk support and separation layers are from the same selective material.[9,70] Also, it requires highly rigorous NIPS condition optimization to obtain an ultra-thin, defect-free skin layer in IAS membranes, which has so far been successful only on a limited number of commercial polymers, like PSF, polyimide (PI), polycarbonate (PC), poly(vinylidene fluoride) (PVDF), cellulose acetate (CA), polyphenylene oxide (PPO) and so on, that mainly target the diffusivity–selectivity dominated gas separations.[67,69,71–74] It appears to be immensely challenging to transfer the IAS membrane design to CO_2/N_2-favored materials, while the TFC strategy at this stage is simply much more facile and flexible. Currently, all post-combustion CO_2 capture membrane systems that reach the pilot scale or beyond as discussed in Section 2.2 are designed as TFCs, demonstrating a huge step forward from lab-scale thick films towards a more practical configuration. On the other hand, hundreds of advanced selective layer materials have been explored in centimeter-to-decimeter-size lab-scale TFC designs, of which

many have actually shown much more superior performances than these commercial developments but only a few ever go beyond the bench scale. Fig. 4 gives a summary of the CO_2/N_2 separation performance of representative TFC membranes from lab to commercial scale, which illustrates this gap pretty well. Clearly, there still exist many technical hurdles that slow down the progress of this transformational membrane technology.

5. Challenges in advancing TFC membranes

5.1. Inconsistency in thin-film and ultrathin-film production

The first challenge is the difficulty of consistent thin-film production. Despite the multitude of existing selective layer materials explored, including the many emerging classes of nanostructures, polymers are still by far the most stable and processable ones with relatively reproducible gas separation performances. Scalable coating methods including dip coating, spray coating and knife/blade/bar casting are highly compatible with polymer solutions.[30,75,76] In contrast, fabricating inorganics, framework structures or 2D laminate nanosheets into ultra-thin films, even with a robust support, requires extremely rigorous control of the *in situ* growth environment or careful tuning of the deposition conditions using some of the much less scalable and more strenuous techniques, such as spin coating, vacuum filtration or vapor deposition.[77–79] The batch-to-batch consistency of the quality of such nanostructure-based thin films is extremely difficult, if not impossible, to maintain. Creating nanocomposite hybrid membranes utilizing flexible polymer matrices is a potential strategy to explore these nanostructures in TFC design, but the size of aggregated nanoparticles is often too big to be contained in a defect-free manner by an ultra-thin polymeric film.[80,81] Reducing the size and promoting uniformity of the nanoparticle could be a strenuous task.

Even for polymers, especially the less mechanically stable rubbery ones, at the ultra-thin state (<100 nm) their dense films could start to lose integrity and generate pinhole defects that destroy their selectivity.[23,82] Applying an additional protective cover, for example, another PDMS layer, on top of the delicate ultra-thin selective layer is one effective strategy to counter the defects.[24] However, not only does it introduce extra transport resistance that reduces the overall CO_2 permeance, it also increases the burden for upscaling given the extra coating step. This inconsistency or reproducibility issue poses a huge constraint on the scalable potential of TFCs, especially for designs that use new-generation materials, and should start to be assessed as part of the overall performance metrics of a TFC design in the future.

5.2. Thickness-dependent gas transport properties

The second challenge is the lack of systematic understanding of the intrinsic property variation at the ultra-thin film state. The

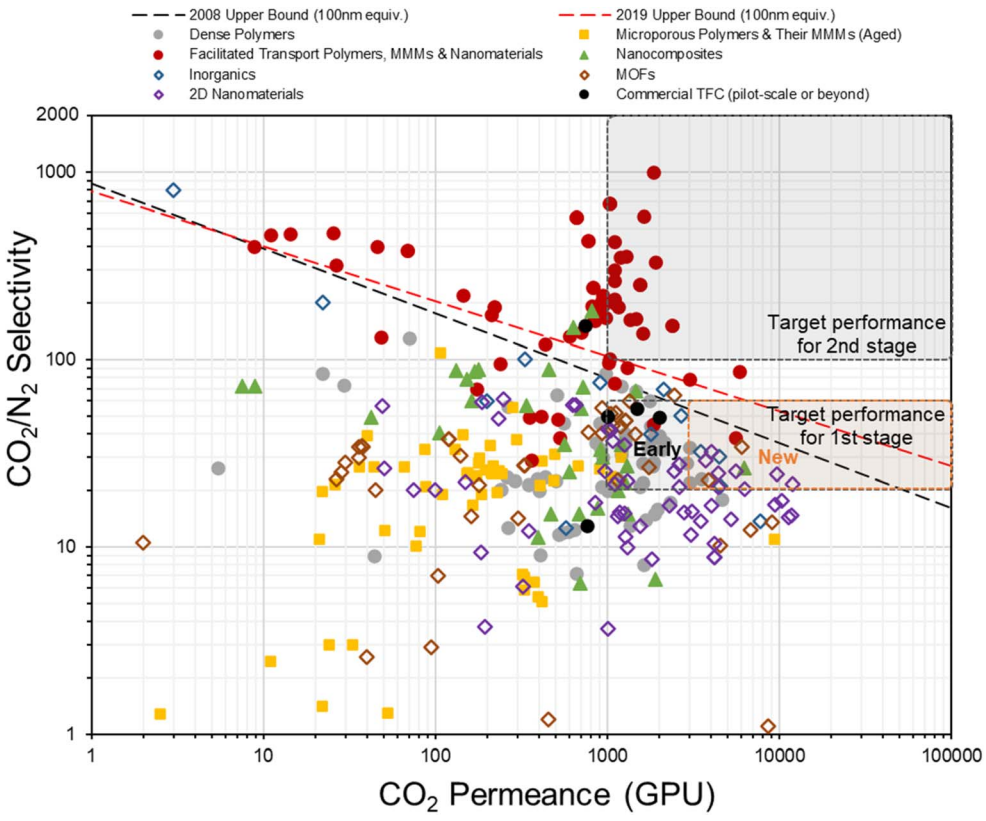

Fig. 4 Summary of the CO_2/N_2 separation performance of existing representative TFC membranes against the hypothesized thin-film upper bounds (assuming 100 nm thickness[9,28]) and proposed industrial targets.

fundamental transport mechanisms for membrane gas separation were developed upon thick dense polymeric films that generally assume a thickness-independence of their intrinsic gas transport properties.[10,12,15] That is widely adopted by most of the gas separation membrane studies and indeed holds true in the so-called "dense thick" regime (several to tens of micrometers). However, when it comes down to thin films, a number of polymers that show great potential and high intrinsic performance for CO_2/N_2 separation experience thickness-dependent permeability deterioration. For example, high free-volume glassy polymers, like PIM and PTMSP, whose intrinsic CO_2 permeabilities are among the highest ever, experience substantially accelerated physical aging at the thin-film state, so much so that up to 90% or more of their permeability could be lost within several days, causing their resultant TFC membranes not to be able to maintain a high CO_2 permeance after standing.[83–85] Incorporating rigid nanoparticles like MOFs was found to be an effective way to counter the aging effect in PIMs and PTMSP, but it tremendously increases the difficulty for defect-free thin-film fabrication and also adds to the production cost.[49,86] Similarly, CO_2-induced plasticization is also more severe in thin films than in thick films, making it another major constraint that limits the performance of thin-film microporous polymers.[9,24]

Another key material used in CO_2/N_2 TFC designs whose permeability shows thickness-dependence is the PDMS. With an intrinsic permeability of >3000 Barrer, a thin PDMS gutter layer that is usually made only 100–200 nm thick in a TFC membrane should theoretically reach a CO_2 permeance above 10 000 GPU, which is a more desirable level of CO_2 permeance in gutter-coated substrates. Yet, most existing thin-film PDMS-coated substrates could only deliver a CO_2 permeance in the range of 3000–5000 GPU, way below the theoretical value.[20,23,46,87] Many reports inclined to attribute this discrepancy to the pore penetration by PDMS, but a few empirical studies actually discovered the thickness-dependence of PDMS.[88–90] In those studies, the permeability of PDMS was found to decrease with the film thickness below a certain thickness threshold. They considered such a phenomenon to be associated with the non-equilibrium sorption–desorption process occurring at the membrane interfaces for thinner films which caused the measured "apparent" permeability to deviate from the intrinsic or "true" permeability.[90] More research attention should be paid to the mechanistic revelation of membrane transport behaviors at the ultra-thin realm in order to generate greater theoretical understanding and more frameworks for thin-film membrane design.

5.3. Geometric restriction and pore penetration

Besides the aforementioned issues, the porous substrate surface also presents some interesting design challenges for TFC membranes, including the geometric restriction and pore penetration. Studies revealed that when the thickness of the selective layer was reduced to be comparable to the surface pore size of the substrate, the gas permeance of the TFC membrane stopped being further enhanced and, in some cases, even started to decrease.[20,82,91] Such a phenomenon is explained by the geometrically limited access of diffused gas penetrants into the substrate surface pores, which caused their diffusion pathways through the selective layer to become detoured/bent and be no longer aligned with the ideal vertical diffusion streamlines as shown in Fig. 5a and b. This geometric restriction phenomenon results in the average effective diffusion length for gas penetrants to travel to the substrate pores being much longer than the apparent thickness of the selective layer, leading to a higher transport resistance.[82] Such an issue could be alleviated by applying a gutter layer with low transport resistance in between the substrate and selective layer because its presence helps keep the effective penetrant diffusion length in the thin selective layer similar to its apparent thickness (Fig. 5c). At the same time, most of the detoured diffusion near the substrate surface will occur in a low-resistance medium rather than in the barrier selective materials. This adds another critical function of the gutter layer in the TFC design.

However, not all selective materials, especially the hydrophilic PEO-based polymers, prefer the presence of a gutter layer because PDMS, as the most commonly used gutter layer material, is highly hydrophobic with poor surface wettability and coating adhesiveness.[92,93] Another way to reduce the geometric restriction effect is through the optimization of the surface pore structure of the substrate which will be discussed more in a later section. Pore penetration, on the other hand, is a more straightforward phenomenon which can be mitigated by pre-wetting the substrate surface pores or, again, by applying a high-permeance gutter layer.[94–96] Completely eliminating this

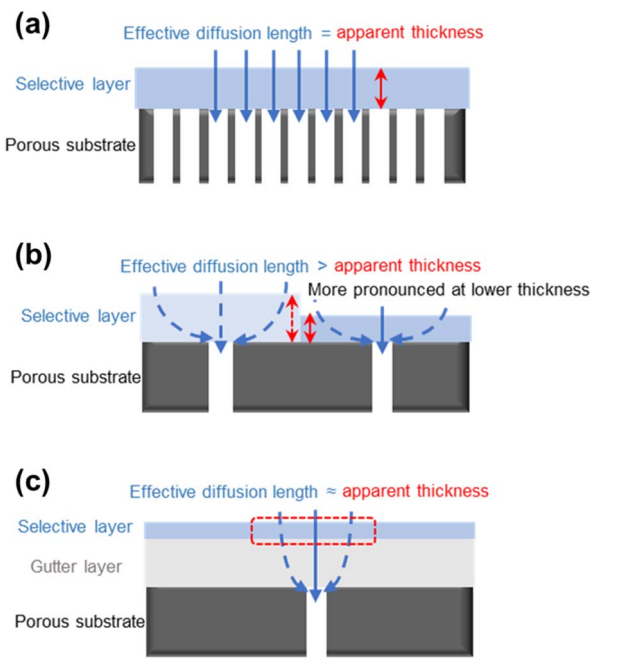

Fig. 5 (a) Theoretical gas diffusion path through the selective layer without geometric restriction. (b) Actual gas diffusion path under the effect of geometric restriction. (c) Alleviation of geometric restriction by the gutter layer.

problem is, however, practically impossible given the fact that the solution-coating method prevails in TFC designs.

5.4. Insufficient translational knowledge and experience

In addition, the lack of systemic knowledge about the translation of available TFC materials into large-scale modules is also a key barrier to their upscaling progress. Scaling up a lab-scale TFC design requires much more than just having a sufficient performance and stability. Mass producible substrates, large-scale coating lines, efficient module assemblies, pilot system design and many other elements must be in place. The stringent handling requirements posed by some of the steps above could easily preclude a huge chunk of lab-exclusive delicate materials. The design of each of these components is heavily experience-based and very often proprietary information such that systematic collections of their design principles and knowledge sharing are very little, if not absent. In addition, the separation efficiency at a larger scale will almost invariably deviate from that obtained under the lab-scale conditions because of unavoidable defect formation in mass production. Right now, most TFC membrane studies claim performances tested over the bench to be above the industrial target, which is very likely to be an overestimate. It is highly advisable for more researchers to conduct correlational studies that could aid in the projection of large-scale performance from lab-scale testing such that proper performance margins could be devised when conceiving a new TFC membrane design from the bench. It is never a setback to realize obstacles against any technological development. After all, the first thing in really solving a problem is to recognize there is one, and in the case of TFC membranes, only by bearing these practical constraints in mind can more effective design strategies be devised with better scalable potential.

6. Reviewing existing TFC membrane design criteria

As a multilayer composite structure, each component in a TFC membrane bears its own sets of functions and hence stipulates different design targets. In this section, the existing materials design criteria widely adopted in most TFC membrane studies will be reviewed in light of the technical challenges delineated above. Potential key areas for further research are also envisioned here.

6.1. Porous substrate

6.1.1. Organic and inorganic porous substrates. As discussed earlier on, the porous substrate in a TFC membrane is there to provide sufficient mechanical support for the thin selective layer while as small resistance as possible against the overall gas permeation. Anisotropic/asymmetric polymeric substrates with a porous skin layer fabricated *via* NIPS using low-cost commercial polymers, such as PAN, PES and PSF, dominate the TFC membrane research.[9,20,24] Besides the cost factor, these flexible polymeric substrates also offer many production and operational advantages including affordability for large-scale fabrication, versatility to be processed into different configurations (*e.g.* flat sheets and hollow fibers), long lifespan and satisfactory resistance against common flue gas contaminants.[20,97,98] Depending on their surface pore structure, polymeric substrates could deliver a CO_2 permeance typically in the range of 50 000 to 100 000 GPU and sometimes even higher to minimize resistance to the overall gas transport according to the resistance model. However, one key constraint of polymeric substrates is their vulnerability towards many organic solvents commonly used for membrane casting, such as dimethylformamide (DMF), *N*,*N*-dimethylacetamide (DMAc), *N*-methyl-2-pyrrolidone (NMP) and dichloromethane (DCM).

Porous substrates fabricated from inorganic materials, like ceramics (*e.g.* α-Al_2O_3) and stainless steels, are also available and often used in TFC membranes designed with delicate nanostructure-based selective layer materials, including, for instance, inorganics and framework materials.[39,99] Inorganic supports usually have better tuned pore size with a highly uniform distribution (*i.e.* nearly isotropic) owing to their compatibility with well-controlled pore forming techniques like etching.[100–102] Also, they possess high thermal stability and are essentially inert towards most solution environments. These features make inorganic supports a good substrate material for growing and fabricating ultra-thin MOF or inorganic selective layers given their demand for a highly controllable synthesis/deposition environment. However, compared with polymeric substrates, porous inorganic supports are much more costly to mass-produce, have poor mechanical flexibility and lack configurational tunability. Although some ceramic materials could be fabricated into anisotropic hollow fiber membranes, they could be too brittle to be considered as a usable support material for TFCs, and also, their material costs are too high for a massive volume process like post-combustion CO_2 capture.[103] Therefore, TFC membranes using nanostructure-based selective materials supported on inorganic substrates could be arguably regarded more as a materials concept-proving or ideal performance benchmarking study with no scalability factor being revealed at this stage. Conversely, polymeric substrates not only are a good research material but also find predominant usage in commercial TFC membrane projects.[27–31] Therefore, another direct advantage of using polymeric substrates for research is that it aligns with the actual commercial configuration and could provide immediate lab-scale verification.

6.1.2. Substrate surface pore structure. Given the porous nature of the substrate, its gas transport characteristics are not determined by the intrinsic separation properties of the constituting materials, be it polymers or inorganics. Rather, it is the internal substrate structure, *i.e.* surface pore size, porosity (per unit porous area), tortuosity and thickness, that dictates its transport resistance. In general, high porosity with smaller pore size (within the Knudsen diffusion regime) is most desirable for a good substrate design because the former can keep the resistance as low as possible while the latter could minimize the effect of pore intrusion.[24,82] At the same time, a relatively smooth surface could be maintained for the subsequent deposition of the selective layer. Higher porosity also offers the advantage of reduced geometric restrictions as the gas penetrants are able to

take a shorter detour to reach a surface pore, allowing their effective diffusion length to be similar to the apparent thickness of the selective layer. However, the trade-off from a high porosity is the increased susceptibility for pore intrusion. Therefore, an optimal substrate pore structure requires a balance between how small the pore size is and how porous the entire surface is. Many existing CO_2/N_2 TFC membrane studies utilized polymeric substrates with a pore size of <100 nm and a surface porosity ranging from around 0.01 to 0.1. Nevertheless, these are very empirical numbers based mostly on prior experiences, rather than systematic investigations on the structure–property relationship due to the lack of such studies to date. There are also studies reporting substrates with surface porosity outside these arbitrary ranges.[76,87,104] It would be of keen interest to the membrane community to see more in-depth research, preferably aided by rigorous simulation and modelling of pore penetration, on the effect of substrate morphology and pore structure on the overall TFC properties.

6.1.3. Challenges and emerging design strategies for TFC substrate development. Besides the low resistance against organic solvents, other constraints exist in the design of efficient substrates. Firstly, despite being a porous medium with Knudsen flow through its skin layer and continuum and viscous flow through its bulk support, the substrate could still contribute a significant amount of resistance to the overall gas permeation, especially as thinner and thinner selective layers are being produced nowadays.[5,105] From the resistance model viewpoint, with a reduced selective layer thickness and hence transport resistance without changing the substrate, the resistance contribution from the substrate to the overall gas permeation becomes increasingly considerable. Studies even reported more than 75% of total permeation resistance being contributed by a porous PSF substrate in a two-layer TFC design as the selective layer thickness gradually decreased.[105] Therefore, permeance gain by reducing selective layer thickness is non-linear and usually less than proportional. Such an effect is more strongly felt by the fast-permeating species (*i.e.* CO_2) than the slower-permeating species (*i.e.* N_2) because for the latter the selective layer resistance is still dominating. This disparity would also result in a reduced overall TFC selectivity when the selective layer becomes too thin. From a transport behavior perspective, the effect of geometric restriction is a key reason that causes the increased resistance contribution from the substrate at low selective layer thickness because the bending of gas diffusion pathways and concentration streamlines occurred primarily around the surface pores on the substrate.[82] Therefore, new TFC designs considering further thinning the selective layer or using ultrapermeable materials should be perceived together with a judicious reduction in the resistance contribution from the substrate through modifying its skin layer thickness and surface pore structure.

Another challenge for the substrate design lies in its fabrication. For polymeric substrates, pore structure inconsistency is an inherent issue posed by the NIPS-based fabrication method because of the lack of precise microscopic control over the phase inversion process. Factors like dope solution formula, coagulation conditions, non-solvent choice and more are all critical to the formation of a desirably porous skin layer with uniformly sized surface pores.[106–108] Even using well-established commercialized production protocols, polymeric substrates are still often produced with an appreciable variance in their surface pore size that tends to yield an unsmooth top surface unconducive for further coating. This is one of the main reasons why TFC membranes for CO_2/N_2 separation are often reported with quite scattered separation performances even using an almost identical combination of selective, gutter and substrate materials.[53,109,110] For example, PAN is a more predominantly used polymeric substrate material than PES and PSF in TFC membrane studies partly because PAN substrates are usually obtained with a better control over their pore size distribution than the others, which could provide more consistent overall TFC performance.[9,24] Some common strategies to modify the substrate fabrication process for generating a more favorable surface pore structure include (1) decreasing the concentration of the polymer dope solution to enhance porosity, (2) incorporating pore-forming additives like polyethylene glycol (PEG) or polyvinylpyrrolidone (PVP) in the dope to create extra porosity, and (3) using block copolymers with self-assembling properties to form segregated microphases that could be selectively dissolved to promote the formation of small and more regularly sized pores.[111–114] Polystyrene-*b*-poly(4 vinylpyridine) diblock copolymer is one such block copolymer that has been fabricated into porous substrates with a highly uniform pore size of ~10 nm.[114] Our own experience working with PAN-based TFC membranes also suggested that substrates made from PAN copolymers consisting of acrylonitrile (AN) and methyl acrylate (MA) units offer better and more consistent performance than homopolymers.

One emerging area to explore for substrate fabrication is nano-to-micron-scale 3D printing which offers more precise manufacturing control and potentially more favorable pore structures. A variety of commercial and lab-synthesized polymers, such as polylactic acid (PLA), polyethylene terephthalate (PET), polyamide (PA), PVA, PDMS, PVDF, PIM-1 and so on, have already been explored as 3D printable membrane materials either for the support or the selective layer.[115–118] However, the substrate pore size obtainable by 3D printing is currently limited by the state of printing technology, which generally falls in the range of several tens to hundreds of micrometers. Advancement in precise and affordable nano-scale 3D printing technology for porous membrane production could be a game-changer for the TFC substrate design.

For the pore intrusion issue, many post-processing techniques have been developed to reduce or minimize it, such as pre-wetting the surface pores with immiscible solvents, annealing the substrate to reduce pore size, quenching the solution to increase viscosity, applying a gutter layer, post-pore opening, and pore sieving using a swelling solvent.[94,95,119–123] However, additional processing steps inevitably would create extra burden for upscaling and have to be considered with caution. Fig. 6 provides an overall summary of the key important considerations and suggestions for substrate design brought forward in this section.

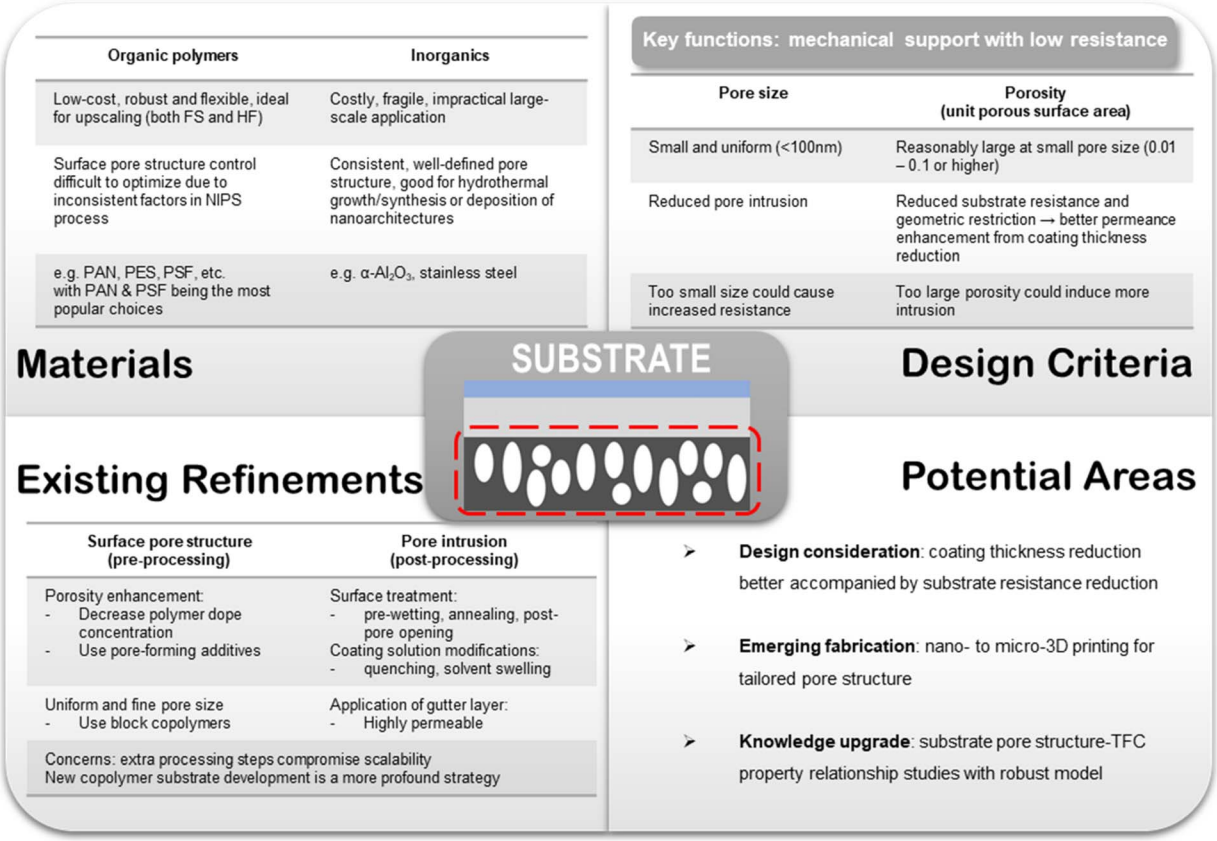

Fig. 6 Design summary for the porous substrate layer.

6.2. Gutter layer

6.2.1. Design criteria for the gutter layer and its relationship with the substrate. The gutter layer is an interlayer placed in between the porous substrate and the selective layer for a number of purposes, including (1) protecting the substrate from the destructive organic solvents used by some selective layer materials, (2) preventing pore penetration by the dilute selective layer coating solution, (3) providing a smooth surface for more uniform and thinner coating, and (4) reducing geometric restrictions to maximize the permeance enhancement by reducing the selective layer thickness. Gutter layers are to be made with as high permeances as possible (*i.e.* made ultrathin or with high intrinsic CO_2 permeability) in order to minimize their additional transport resistance. This criterion is especially critical for gutter layers made with solution-processable dense polymers which are the most prevalent type of gutter layer material used in both commercial and lab-scale TFC designs for CO_2/N_2 separation. More specifically, because pore penetration and geometrically restricted bending of gas diffusion pathways are also inevitable for polymer-based gutter layers deposited *via* solution-coating, using polymers with a high intrinsic gas permeability could mitigate the additional transport resistance arising from these issues. On the other hand, the selectivity requirement for the gutter layer is usually much more lenient (~3–11) because the molecular partitioning primarily takes place in the selective layer.

Simulation studies conducted by Kattula *et al.* revealed that the presence of the gutter layer could exert a critical impact on the overall gas transport properties of the TFC membrane.[82] As compared with a two-layer design comprising only the porous substrate and a thin selective layer, it has been shown that the introduction of a highly permeable gutter layer allowed a greater permeance enhancement effect to be achieved by the same extent of selective layer thickness reduction owing to the suppression of geometric restriction. They also corroborated the significant effect of substrate surface pore structure on the TFC performance. Larger porosity was found not only able to promote more geometrically unrestricted gas diffusion in the two-layer TFC design but also amplify the extent of separation performance enhancement from a high permeance ratio of the gutter layer to the selective layer (*i.e.* using a highly permeable gutter material) in a three-layer design. Another profound criterion suggested by this study is that a gutter layer thickness similar to the mean substrate surface pore diameter would be optimal, which could maximize the overall performance enhancement by the gutter layer without introducing excessive transport resistance. However, the simulated TFC system is based on the assumption of zero pore penetration which is unrealistic for an actual TFC design. Future studies capturing the effect of pore penetration would be very helpful to provide a more rigorous assessment of the impact of the gutter layer. Nevertheless, despite these existing preliminary guidelines for

a three-layer TFC design, most current TFC studies are usually performance-driven based on serendipitous discoveries such that they only retrofit the results to matchable guidelines rather than depend on them for initiating the discoveries.

6.2.2. Highly permeable polymeric gutter layer materials. In terms of materials, the two most commonly used polymers for producing the gutter layers are PTMSP and PDMS. The former is a glassy polymer with extremely high free volume (up to 0.38) and a high intrinsic CO_2 permeability of over 19 000 Barrer.[25,124,125] In a TFC configuration, studies showed that the PTMSP gutter layer could obtain an astounding CO_2 permeances of ~18 000–20 000 GPU at a low CO_2/N_2 selectivity of ~3 when freshly made.[83] However, as discussed before, due to their fast physical aging rate especially in a thin-film state, such high permeances are only a transient number. The aging-stabilized CO_2 permeance of PTMSP gutter layers is usually only around 10% of the original, making it a less practical choice compared with PDMS.[9] Strategies to mitigate physical aging are so far largely limited to the incorporation of rigid nanoarchitectures to suppress PTMSP chain relaxation, such as graphene, GO, or porous aromatic frameworks (PAF).[126,127] However, despite showing some effectiveness, the modified PTMSP mixed-matrices still experienced significant aging with unsatisfactory stabilized CO_2 permeance. The added scalability constraint of fabricating thin-film nanocomposites (TFN) is also an insurmountable challenge faced by such aging mitigation scheme. PDMS is a rubbery polymer with also a very high intrinsic CO_2 permeability typically between 3000 and 4000 Barrer but a higher CO_2/N_2 selectivity of around 10–11.[19,46] It possesses a robust film-forming ability, excellent solvent stability especially after crosslinking, and low surface energy due to which it can be easily attached to most surfaces. More importantly, PDMS has no aging issue and has cheap commercial availability that makes it an ideal and the most popular gutter layer material for post-combustion CO_2 capture TFC membranes so far. Similar to the selective layer, the PDMS gutter layer is generally applied *via* a number of coating techniques, such as dip coating, spray coating, spin coating or blade casting, which can usually lead to a dry thickness of around 100–200 nm without defects.

One of the design limitations for PDMS gutter layers is the significant deviation of their apparent CO_2 permeance from ideality at low thicknesses. Based on early discussions, such an under-performance is most likely a compounded effect from the thickness-dependent permeability of PDMS, pore penetration and geometric restriction, whereas most existing studies usually attribute it to just one of these factors. Therefore, reducing the PDMS layer thickness often yields less than proportional or even marginal CO_2 permeance enhancement and could eventually reach a limit of around 100 nm, below which defects will start to form even using the current state-of-the-art dip-coating techniques.[46,89] Most of the existing PDMS-coated TFC substrates could only obtain a CO_2 permeance of around 3000–5000 GPU whereas a CO_2 permeance of >10 000 GPU is desired to maintain a high overall performance and meet the new industrial metrics (>3000 GPU) after subsequent coatings. Theoretical calculations based on a simplified resistance model revealed that an order of magnitude higher CO_2 permeance in the support (*e.g.* from 10^3 to 10^4 GPU) could allow the same selective layer to deliver almost an order of magnitude higher overall permeance.[52] So far, only a few studies reported pristine PDMS gutter layers with a CO_2 permeance >10 000 GPU. One of them attributed the high CO_2 permeance to a combined effect of ultra-thinness (~100 nm), minimal pore intrusion, and an extra-porous support with finely sized surface pores (~0.2 porosity and ~40 nm pore diameter).[87] Another study fabricated free-standing PDMS ultra-thin films with a thickness of as low as 34 nm using a sacrificial support and obtained a record CO_2 permeance of over 40 000 GPU while maintaining the intrinsic selectivity.[88] However, their method requires a careful secondary transfer step to place the film onto a substrate which lacks process scalability and is thus only meaningful for research purposes. Nonetheless, reducing the thickness of the PDMS layer has proven to be still an effective strategy to push its permeance above the range of industrial interest at the risk of defect formation. Therefore, advancements in both defect-free ultrathin-film PDMS deposition technologies and our fundamental knowledge about how to overcome the thickness-dependence of its intrinsic separation properties would be of monumental value to the development of commercializable high-performance TFC membranes.

In the meantime, improvement in the intrinsic permeability of its constituting materials should be concurrently explored. A few materials modification strategies have been attempted to boost the performance of the PDMS thin layer which include (1) introducing CO_2-philic moieties like PEO into the PDMS polymers *via* block copolymerization or physical incorporation, and (2) incorporation of nanoporous architectures like MOFs that could provide additional fast diffusion pathways through their open cavities or enhance the preferential adsorption of CO_2 over N_2.[128–131] In order not to jeopardize the processability, nanofillers that are molecularly compatible and soluble in the same solvent should be pursued.

6.2.3. Emerging gutter layer materials. Other emerging gutter layer materials with more favorable gas transport characteristics towards the CO_2/N_2 separation have been explored, including fluoropolymers, like Teflon AF2400, and frameworks or nanostructures, like MOFs, COFs and nanofibers.[40,129,132] The former demonstrated an ultrathin-film forming ability (<100 nm) without incurring significant thickness-constrained permeance enhancement or defects, but its super-hydrophobic nature and extremely low surface wettability make rigorous surface modification techniques (*e.g.* plasma treatment) necessary in order to be better compatibilized with the selective layer. The latter, on the other hand, could deliver extraordinary CO_2 permeances in the range of a few tens of thousands with a low but usable CO_2/N_2 selectivity owing to their intrinsically porous nature that allows for rapid gas diffusion. Another advantage of nanostructure-based gutter layers is their better surface wettability/hydrophilicity than the inherently hydrophobic PDMS partly arising from their rougher, irregular crystalline surface morphology, allowing easy adhesion of CO_2-philic polymers (mostly hydrophilic in nature) on top of them. These delicate crystalline thin films, however, simply lack any meaningful practicality at this stage due to their mechanical

instability and strenuous fabrication/growth process. Compared with these new materials, PDMS still offers the distinct and currently unsurpassable advantage of scalable and low-cost fabrication.

6.2.4. Considerations for gutter-free TFC design. One last note on the gutter layer design is about its industrial implication. While a three-layer design is becoming increasingly prevalent, a two-layer design is, from an industrial viewpoint, still more preferable because the reduced number of coating steps involved in a fewer-layer design would undeniably make its mass production simpler and less costly. Despite the pore penetration issue faced by direct selective layer coating, post-treatment strategies like those mentioned earlier on in this section have shown great potential for mitigating this problem. In addition, modifying the coating technique or coating solution could also be effective counter-measures. For example, a large-scale spray coating technique was developed by Jiang *et al.* that could achieve atomized deposition of a coating solution on a flat sheet porous substrate with a much shorter curing time and hence minimal intrusion.[76] On the other hand, coating solutions containing polymer solutes with crosslinked networks or an extremely high molecular weight could also possibly reduce pore penetration by forming interconnected bridges over the surface pores.[24,54] Besides, emerging 2D nanosheet-based selective layer materials with high aspect ratios, usually deposited *via* vacuum filtration or spin coating, like GO, are less troubled by the pore penetration issue owing to their large flake size.[133–135] Although they have low scalability at the current state, the message behind these novel materials is to show that pore penetration may not be as insurmountable as people thought. Therefore, future research in reducing existing high-performance three-layer designs into a two-layer one would make great industrial sense. A summary of the key design criteria and suggestions for the gutter layer is provided in Fig. 7.

6.3. Selective layer

6.3.1. Design criteria for the selective layer. The selective layer is essentially a thin or ultra-thin film made of materials with high intrinsic CO_2/N_2 separation performance that governs the overall separation efficiency of the TFC membrane. As a barrier layer with high transport resistance, selective layers, especially those produced from dense polymers, are to be designed as thin as possible in a defect-free manner, which has been one key research objective for TFC membranes for long. While materials with both high intrinsic CO_2 permeability and CO_2/N_2 selectivity are definitely good selective layer candidates, the TFC configuration and actual process driving-force constraint could actually alleviate such performance requirements, respectively. The former allows materials with a relatively low permeability to deliver high permeance by reducing their thickness, while the latter imparts a very high selectivity not particularly important for post-combustion CO_2 capture which operates within a pressure-ratio-limited regime. For example, Pebax® and Polyactive™ are two of the most widely used commercial PEO-based block copolymers for producing selective layers in TFC membranes for CO_2/N_2 separation owing to their sufficient CO_2/N_2 selectivity of ~20–60.[136–138] Despite having an intrinsic permeability of only around 100–200 Barrer, these two copolymers could achieve a CO_2 permeance over 1000 GPU in a TFC configuration.[54,136] Therefore, it is equally important to assess how scalably and controllably a material can be made into thin-films while advancing its separation performance. In fact, progress in intrinsic performance or thin-film production is mutually beneficial because the enhancement of one would ease the design constraints for the other. Of course, enhancement in both performance and production is always the ultimate goal for TFC research.

Unlike the substrate or gutter layer with a limited range of applicable materials, hundreds of different materials or hybrids have been explored as the selective layer given the versatility of TFC design, ranging from numerous PEO-based, amine-containing, interfacially synthesized, microporous polymers and their nanoparticle-incorporating hybrids to the vast selections of frameworks, inorganics and carbon-based nanoarchitectures. Tables 1 and 2 summarize the CO_2/N_2 separation performance and the respective target enhancement mechanisms of a number of representative TFC materials from each category. It is worth mentioning that this table is definitely not an exhaustive list given the huge pool of materials, which have been comprehensively reviewed elsewhere.[9,18,20,24] The key purpose of the following discussions is to bring forward some of the important design factors/constraints that are paid less attention to among the existing performance-oriented studies.

6.3.2. Solubility selectivity *vs.* diffusivity selectivity in membrane CO_2/N_2 separation. For polymer-based selective layer materials, they usually possess high CO_2 solubility from their CO_2-philic functionalities or high fractional free volume that facilitates CO_2 sorption. Their separation performance is hence dominated by the solubility selectivity of the condensable CO_2 gas over the permanent N_2 gas. Despite having a high CO_2 solubility, plasticization is a less prominent issue than physical aging in TFC membranes developed for post-combustion CO_2 capture presumably due to the very low CO_2 partial pressure in the feed. Also, more and more studies showed awareness to test the long-term performance stability of their TFC membranes which could provide an assessment of the impact of the CO_2 solvation effect after long-term exposure. On the other hand, although there is a kinetic diameter difference between CO_2 and N_2, diffusivity–selectivity based on a size sieving mechanism is a much less explored factor in CO_2/N_2 membrane designs. Polymeric materials reported with very high CO_2/N_2 permselectivities, like PEO-based polymers and amine-containing facilitated transport membranes (FTM), almost exclusively rely on the preferential sorption or reaction of CO_2 with the underlying polymers to obtain a high solubility selectivity.[48,55,149–151]

Nanostructure-based selective materials, like MOFs, zeolites or GO, which are known to be highly molecular-sieving owing to their well-defined subnano-scale apertures or channels, mostly showed similar CO_2/N_2 permselectivities in the range of ~20–70 to the advanced polymeric materials, shown in Table 2. Those that demonstrated extremely high selectivities (over a few hundreds) were mostly either modified with amine-containing

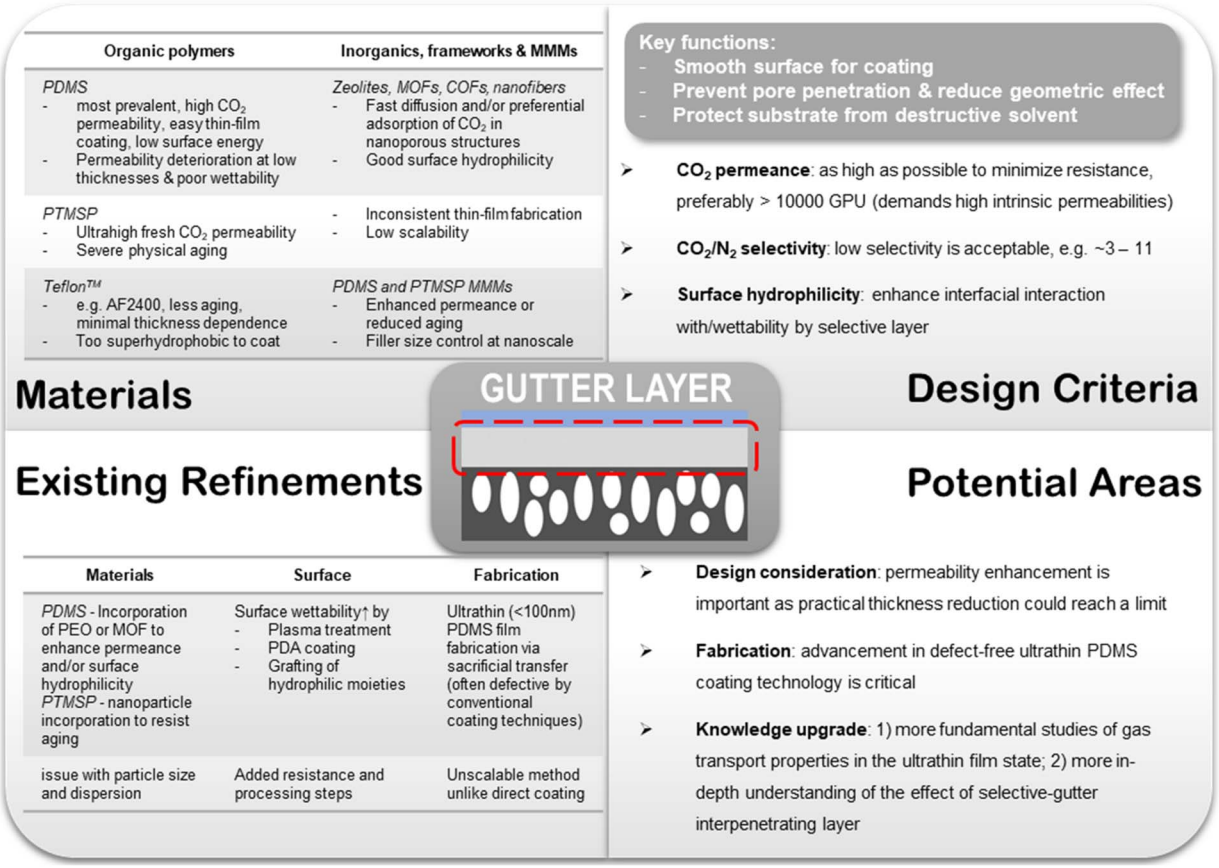

Fig. 7 Design summary for the gutter layer.

transport-facilitating moieties or exhibited preferential CO_2 adsorption properties, rather than size-discrimination.[38,99,133–135] In contrast, membrane CO_2/CH_4 separation (with merely a 0.16 Å bigger gas pair size difference than CO_2/N_2) is often dominated by materials with high diffusivity selectivity (*i.e.* size-sieving ability), including those nanostructure-based ones mentioned above and other novel glassy polymers with strongly size-sieving ultramicropores generated from rigid polymer backbones or thermal treatment, like PIMs, thermally rearranged (TR) polymers and carbon molecular sieves (CMS).[18,21,175–177] This reveals the difficulty in transferring membrane design from one application to another even with a small difference in the partitioning targets. Some of the TR polymers also showed excellent CO_2/N_2 separation performance owing to their microporosity for preferential CO_2 sorption and fast diffusion, but they are all produced as integrally skinned asymmetric membranes using a single polymer, followed by thermal treatment of the entire membrane.[178–180] They can hardly be fabricated in a TFC configuration due to the harsh treatment conditions (>300 °C) that not only will damage the polymeric substrate but is also too energy-intensive to be cost-efficient. Some studies suggested that the lack of molecular sieving between CO_2 and N_2 is due to their similar critical volume, but systematic investigation in that area is lacking.[24] More fundamental research should be carried out to reveal the possibility or potential of molecular-sieving materials development for the CO_2/N_2 separation which could offer a clearer direction for future materials discovery in this field.

6.3.3. Limitations in ultrapermeable and ultraselective polymers for CO_2/N_2 separation. Among all the polymer-based materials with good CO_2/N_2 separation properties, PIMs and FTMs are two special classes particularly worth mentioning because they constitute the most permeable and the most selective end of the performance map. PIMs are able to confer extra-high free volume due to their contorted rigid backbones that prevent efficient polymer packing, which endows them with the highest intrinsic CO_2 permeabilities among all known polymers at reasonable gas pair selectivities. For example, some benzotriptycene-based PIMs could achieve a CO_2 permeability of ~10 000–50 000 Barrer with a CO_2/N_2 selectivity of around 15–20 when freshly made.[21] These results, if translated into a TFC configuration as they are, could easily make the current industrial design targets obsolete. However, as shown in Fig. 4, actual PIM-based TFC membranes mostly showed performances, especially the CO_2 permeance, below the lower end of the industrial target (<1000 GPU) due to their fast aging at the thin-film state. The incorporation of rigid nanoparticles to suppress aging has demonstrated some but quite limited success so far.[86,121] Clearly, a key future research area for PIM-based TFC membranes should fall in the development of anti-

Table 1 Summary of polymer-based TFC membrane materials[27–32,40,48,54–56,83–85,121,128–132,136,139–152]

Materials Class	Sub-class	Materials	Thickness (nm)	Support materials		Feed		Testing conditions		TFC separation performance		Main design targets	Ref.
				Gutter layer	Porous substrate	CO_2/N_2 composition	Humid	Temperature (°C)	Pressure (bar)	CO_2 permeance (GPU)	CO_2/N_2 selectivity		
Polymers	PEO-based	PEG	60	PDMS	PAN	Pure gas	No	35	3.4	1260	40	Selective layer:	[139]
		PEG	54	PDMS/MOF	PAN	Pure gas	No	35	1	1990	39	➢ Increasing ethylene oxide (EO) content to enhance CO_2-philicity and solubility	[130]
		PEG	30	NH_2-MIL-53 (MOF)	α-Al_2O_3	Pure gas	No	35	1	3000	34		[140]
		XLPEG	120	COF-LZU1	PAN	15/85	Yes	25	0.5	1843	28.2		[40]
		Crosslinked PEGMEA	620	None	PEGDA/PEG	Pure gas	No	25	2	1889	39	➢ Copolymerization of PEO with rigid blocks to enhance film forming	[141]
		PEO-Si/PDMS	100	CHN nanofibers	PAN	Pure gas	No	25	2	2860	28		[129]
		Pebax®1074	<1000	PDMS	PVDF (HF)	Pure gas	No	25	1.38	551	46	➢ Suppressing PEO crystallinity to enhance permeability/permeance	[142]
		Pebax®1657	2-20	PDMS	PAN	Pure gas	No	25	3	1200-3500	72-23		[136]
		Pebax®1657	200	PDMS-*b*-PEO	PAN	Pure gas	No	30	3	1768-2142	44-36		[131]
		Pebax®1657	130	ZnTCPP (MOF)	PAN	Pure gas	No	35	1	1710	34		[132]
		Pebax®/PEG-DME500	400	None	PES	20/80	No	57	3.3	1615	8	Gutter layer:	
				Zeolite Y						940	30	➢ Improving permeance or surface hydrophilicity through incorporation of MOF or PEO or surface modification	[56]
		Pebax®2533	890	PDMS	PAN	Pure gas	No	35	3.5	434	23.5		[143]
		Pebax®2533	160	ZnTCPP (MOF)	PAN	Pure gas	No	35	1	1820	27		[132]
		Pebax®2533/PEG	320	PDMS	PAN	Pure gas	No	35	3.4	920	21		[144]
		Pebax®2533/PEG-*b*-PDMS	810	PDMS	PAN	Pure gas	No	35	3.5	1030	21		[128]
		PolyActive™	45	PDMS	PAN	Pure gas	No	30	1	1750	60	➢ Utilizing nanostructures with fast transport properties, e.g. MOFs, COFs, zeolites, nanofibers	[54]
		PolyActive™	600	CoTCPP (MOF)	PAN	Pure gas	No	35	1	900	46		[132]
			150	CuBDC						1600	28		
			100	ZnTCPP						2070	33		
	Microporous polymers	PTMSP/PEI/PEGDEG	-	None	MFFK-1	-	No	22	5	Fresh 18.5-20k	3.6	➢ High permeance from intrinsic microporosity	[83]
		PIM-1	290-420	PTMSP	MFFK-1	Pure gas	No	24	3	Fresh 2.7-8k	55.7-35.8	➢ Aging suppression method development, e.g. nanoparticle incorporation	[84]
										Aged 208-297	56.2-34.6		
		PIM-1	850	None	PAN	Pure gas	No	30	1	Fresh 4320	19		[85]
										Aged 490	31		
		PIM-CD	1317	PDMS	PAN (HF)	Pure gas	No	35	3.4	Fresh 483	22.5		[121]
	Interfacial polymerization	Polyamide	100	None	PSF	20/80	Yes	Ambient	1.1	173	70	➢ Exploiting EO-containing or CO_2-reactive molecules as the aqueous-phase monomers	[145]
		DGBAmE(EO3)/TMC	130	PDMS	PSF	15/85	No	22	5	1264	37		[146]
		DAmPEG(EO21)/TMC	150						1.1	973	84		
		DGBAmE/DNMDA/TMC	<500	PDMS	PSF	15/85	Yes	22	1.1	1600	138		[147]
		DGBAmE/DAmBS/TMC	820	PDMS	PSF	15/85	Yes	25	1.1	5830	86	➢ Interfacial reaction optimization	[148]
	Facilitated transport membranes (FTMs)	PVAm	257	PDMS/PDA	PSF	15/85	Yes	25	1.5	1100	75	➢ High CO_2/N_2 reactivity selectivity from reactive carriers, e.g. amines, assisted by water	[48]
		PVAm	834	None	PSF	10/90	Yes	35	1.1	1840	1000		[55]
		PVAm/PVA	500	None	PSF	10/90	Yes	25	2	210	174		[149]
		PVAm/PG	100	Zeolite Y	PES	20/80	Yes	57	1.515	1100	>200		[150]
		MMP-1 (PVAm-based)	50	PDMS	PSF	15/85	Yes	25	2	5500	38	➢ Inducing ordered microporosity to improve permeance	[151]
		MMP-3 (PEI-based)								3000	78		
	Inorganic polymers	Crosslinked polyphosphazenes	200	PDMS	PAN	Pure gas	No	22	10	1200	31	-	[152]
	Commercial	Polaris™ Gen-1 (demo)	-	-	-	Pure gas	No	21	3.4	1000	50	-	[28]
		Polaris™ Gen-2 (pilot)	-	-	-	Pure gas	No	-	-	2000	49		
		Polaris™ Gen-3 (bench)	-	-	-	Pure gas	No	25	1	2950	50		[29]
		PolyActive™/PDMS (pilot)	85	PDMS	PAN	Pure gas	No	21	3-11	1480	>55		[27]
		2nd Gen PEEK HFM (pilot)	-	-	(HF)	11/89	-	14-23	0.26-0.35	2150-2670	-		[31]
		PVAm (pilot)	185	None	PES	20/80	Yes	57	1	741	151		[30]
		PRISM™ (pilot)	-	None	PSF (HF)	15/85	No	Ambient	1.5	763	13		[32]

aging technology with better effectiveness and practical implementation in order to translate their "ultrapermeability" into "ultrapermeance". It is interesting to note that aging for highly diffusivity–selectivity governed separations like H_2/N_2 and H_2/CH_4 often results in a more than proportional gain in the selectivity than the loss in H_2 permeability, which allows the overall intrinsic separation performance to improve with aging. Several ladder PIMs and polynorbornenes have demonstrated significant aging-induced performance enhancement for these separations.[181,182] However, for solubility-selective separations like CO_2/N_2, selectivity gain from reduced free volume element size is proportionally traded off with permeability loss, resulting in the downward movement of overall performance along the upper bound with aging.

Facilitated transport membranes (FTMs), on the other hand, separate CO_2 from N_2 based on the preferential reversible reactions of CO_2 with the carriers in the membrane in the presence of water. In other words, in facilitated transport, it is the reactivity selectivity that governs the gas discrimination rather than diffusivity or solubility selectivity.[183,184] Amine-functionalities are the most common carrier groups exploited in FTMs because of their high reactivity with CO_2 under humid conditions. Other non-amine-based carriers, like organic bases or mimic enzymes, have also found application in some FTM designs but are less preferred due to their comparatively slower CO_2-reaction kinetics.[18,185–188] In contrast, N_2 or other unreactive penetrants are still permeated *via* the solution–diffusion process with comparatively slower kinetics, allowing an extraordinarily high CO_2/N_2 selectivity to be achievable by FTMs. For example, TFC membranes with a selective layer made of polyvinylamines (PVAm), under humidified conditions, could easily achieve an extremely high CO_2/N_2 selectivity of >100 or, in some studies, reaching several hundreds to a thousand, which are among the highest known for polymers and by no means attainable by solution–diffusion governed dense polymers at the current stage.[55,149,150,157,158] However, as previously established, these exorbitant selectivity values are way above the optimal range for a pressure-ratio-limited separation like flue gas CO_2 capture. The amount of added purity will be very marginal at the expense of dramatic membrane area requirement, unless there is simultaneous enhancement in the permeance with orders of magnitude increment. Yet, as revealed by Tables 1 and 2, most of the "high-permeance" FTM-based TFC membranes currently developed achieve a CO_2 permeance in the range of 1000–2000 GPU which is arguably not a compatible value with their ultrahigh CO_2/N_2 selectivities. Nevertheless, for

Table 2 Summary of nanostructure- and nanocomposite-based TFC membrane materials[23,37–39,41,42,49,80,85,99,127,133–135,153–174]

Materials Class	Sub-class	Materials	Thickness (nm)	Support materials		Feed		Testing conditions		TFC separation performance		Main design targets	Ref.
				Gutter layer	Porous substrate	CO_2/N_2 composition	Humid	Temperature (°C)	Pressure (bar)	CO_2 permeance (GPU)	CO_2/N_2 selectivity		
Nano-composites	MMMs	PEG/SiO_2-PEI-PDA	55	PDMS	PAN	Pure gas	No	35	3.5	1300	27	➢ Incorporation of nanoparticles to enhance permeance, selectivity or both through e.g. fast diffusion pathways, preferential CO_2 adsorption capacity - retard physical aging - reinforce polymer matrix to reduce pore penetration ➢ Modify/decorate nanoparticles with polymers to increase their affinity with polymer matrices or CO_2-philicity	[153]
		PEG/NH_2-MIL-53	4900	None	α-Al_2O_3	Pure gas	No	35	3	560	35		[154]
		PEG/FeDA	45	PMDS	PAN	Pure gas	No	35	3.5	1200	35		[155]
		Pebax®1657/PEA-GO	70	AF2400	PAN	14/86	No	22	2	1455	68.1		[23]
		PolyActive™/MOF	300-500	PDMS	PAN	-	No	35	3	1260	22		[80]
		PTMSP/PAF-11	1700-6800	None	PAN	-	No	25	2	1900	6.7		[127]
		PIM-1/NH_2-UiO-66	850	PDMS/MOF	PAN	Pure gas	No	30	1	Fresh 7460 Aged 900	26 26		[85]
		PIM-1/MOF-74-Ni	860							Fresh 5018 Aged 1200	31 30		
		PIM-1/C-HCP	2000	None	PAN	Pure gas	No	25	2	Fresh 11500 Aged 9300	8 11		[49]
		PVAm/PEG-UiO-66	410	PDMS	PSF	15/85	Yes	25	3	1295	91		[156]
		PVAm/MIL-101(Cr)	200	PDMS	PSF	15/85	Yes	25	5	823	242		[157]
		HMMP-PVAm	180	PDMS	PSF	15/85	Yes	25	2	1544	252		[158]
		PVP7-co-VAc3/MWNTs	-	None	PES	20/80	Yes	57	1	970	167		[159]
Frameworks	MOFs	ZIF-8	550	None	α-Al_2O_3	Pure gas	No	30	1	120-330	37.3-27.2	➢ Open apertures as fast transport channels ➢ Preferential CO_2 adsorption in MOF pores or reaction with ligands ➢ Improving defect-free thin-film production ➢ Reducing MOF structural flexibility	[39]
		ZIF-62	70k	None	α-Al_2O_3	Pure gas	No	Ambient	1	38	34		[160]
		ZIF-67	3000	ZnO	α-Al_2O_3	Pure gas	No	25	1	94	2.9		[161]
		ZIF-67	80k-280k	PDMS/PVA	PSF	15/85	Yes	25	5	2436-6016	64-34		[162]
		UiO-66	3500	None	α-Al_2O_3	50/50	No	Ambient	-	180	21.4		[163]
		PDA/UiO-66	800	None	α-Al_2O_3	50/50	No	25	1	1115	51.6		[164]
		MOF-5	14k	None	α-Al_2O_3	88/12	No	25	4.45	>1340	>60		[165]
		CAU-1	2000-3000	None	α-Al_2O_3	90/10	No	25	1	3880	22.8		[166]
		$Cu(dhbc)_2(bpy)$/GO	100	None	α-Al_2O_3	Pure gas	No	-	2	1144	22.8		[167]
Inorganics	Zeolites	Na-Y	10k-20k	None	α-Al_2O_3 (HF)	50/50	No	30	1	900-2690	75-50	➢ High CO_2 adsorption capacity with fast kinetics than N_2 ➢ Exchanging the constituting cations in zeolites to tune sorption selectivity ➢ Amine-modifying silicas to increase selectivity	[37]
		Na-Y	-	None	α-Al_2O_3/SS	50/50	No	30	1.38	286	503		[99]
		B-ZSM-5	5k-80k	None	α-Al_2O_3/SS (HF)	50/50	No	27	4.5	570	12.6		[168]
		Na-ZSM-5								7760	13.7		
		Rb-Y	3000	None	α-Al_2O_3 (HF)	50/50	No	35	1	1790	40		[169]
		Silicate-1	-	None	SS	50/50	No	20	1	2130	69		[170]
		SAPO-34	6000	None	α-Al_2O_3 (HF)	50/50	No	22	2.4	3500-4500	32-21		[171]
		K-Y	10k-15k	None	α-Al_2O_3 (HF)	50/50	No	40	1	4480	30.3		[172]
	Silicas	Silica	30	Silica	γ-Al_2O_3 (HF)	Pure gas	No	80	6.5	200	60		[173]
		Silica/APS	-	None	γ-Al_2O_3 (HF)	1/99-20/80	Yes	22	1	22-330	100-200		[38]
Carbon-based nanostructures	Graphene	CO_2-philic polymer-functionalized graphene	20	None	Tungsten	Pure gas	No	30	2	630-11790	14.7-57.2	➢ Ultrathin films from laminate stacking with high permeance ➢ Incorporation of CO_2-philic or reactive motifs by functionalization or into interlayer channels to enhance selectivity	[41]
	Graphene oxides (GOs)	GO	<10	None	PES	Pure gas	No	25	0.3	100	20		[42]
		GO-ionic liquid	1050	None	α-Al_2O_3	Pure gas	Yes	20	1	68.5	382		[133]
		GO-piperazine	16	None	PES (HF)	15/85	Yes	80	0.069	1020	680		[134]
		GO-EDA	28	None	PES (HF)	15/85	Yes	75	0.069	660	572		[135]
	Carbon nanotubes (CNTs)	CNT/NCP-TEPA	220	None	PES	15/85	Yes	80	1	1092-1280	356-425		[174]

a two-stage separation unit, the FTMs could be attractive membrane materials for the second stage with a CO_2-enriched feed that entails no pressure-ratio limitation.

Many potential areas are awaiting exploration to make FTM an even more attractive and practical membrane design. Firstly, new FTMs should be designed with higher CO_2 permeance beyond 2000 GPU to match their outstanding selectivity, which could possibly be achieved by exploring the fast diffusion characteristics of porous or 2D nanomaterials through nanocomposite strategies. Secondly, given the fact that flue gas with a reliable or consistent water profile is not ubiquitous and its water content varies from plant to plant, more studies to systematically investigate the relationship between FTM transport properties and humidity conditions are required to reveal clearer guidelines for interpreting the FTM separation performance. For example, most current FTM designs were tested with saturated water at a range of temperatures that often differed from one another, which could very possibly cause deviations from the actual humidity, in particular considering the humidity variation along the membrane modules in industrial applications.[183,184] Also, the requirement of high humidity by FTMs could be an issue for the porous polymeric substrates as studies have shown that long-term exposure to water could lead to its condensation onto and hence the blocking of skin layer pores.[53] These issues should be paid more attention to in future FTM-based TFC designs. Lastly, emerging FTM designs using mobile carriers, like ionic liquids (ILs) and amino acid salts, are definitely worth more attention. ILs are liquid-state organic or inorganic salts with minimal volatility and high CO_2 solubility or reactivity, and those with amine-functionalized cations could be utilized as mobile carriers in FTMs to deliver a higher intrinsic CO_2 permeability and selectivity than their solid-carrier-based counterparts.[189] Similar to ILs, high-performance TFC FTMs have also been produced from non-volatile amino acid salts with high CO_2-reactivity.[190,191] However, given their liquidous nature and relatively low viscosity, the leaching problem remains a barrier against their potential applicability towards TFC development.[18,192] Advancements in thin-film polymeric matrices that could offer a stable containment of liquidous additives would be a valuable research area.

6.3.4. Exploring CO_2-philic motifs *via* interfacial polymerization. Although polymeric selective layers are most commonly deposited *via* a coating technique, direct *in situ* synthesis of

stable ultra-thin polyamide (PA) films on a porous substrate is also feasible through interfacial polymerization (IP) between the amine (in aqueous phase) and acyl chloride (in organic phase) monomers. The IP TFC membranes have already been a commercialized technology for reverse osmosis (RO) water desalination for over two decades with high technological maturity.[193–195] Exploring the transferability of the IP technology for gas separation is nothing but a reasonable move. While studies showed that IP TFC membranes synthesized using conventional PA monomers were unable to obtain attractive CO_2/N_2 separation performance, CO_2-philic groups like PEO or CO_2-reactive amine-containing motifs could be incorporated into the PA layer to achieve promising, multifaceted performance enhancements by substituting the aqueous monomer.[145–148] This makes the IP membrane a highly versatile platform for exploiting novel monomers with potentially excellent CO_2/N_2 separation properties, especially those that find it difficult to form thin-films otherwise. Nevertheless, one possible limitation faced by IP TFC membranes for gas separation is the large-scale defect control because the defect tolerance for gas separation is much smaller and more stringent in terms of pinhole size than for water applications.

6.3.5. Non-polymer based and nanocomposite selective layer materials. Selective layers made entirely from 3D nanostructure-based materials like MOFs and inorganics arguably only have research demonstration purposes at the current stage because of their mechanical instability, stringent *in situ* synthesis/growth conditions and the fact that a majority of such designs are only realized on brittle and expensive ceramic substrates. Besides, the susceptibility of crystalline materials to form extrinsic defects at grain boundaries or between crystalline domains poses a severe performance reproducibility issue.[45,52] Applying these materials as the entire gutter layer would face similar constraints as discussed earlier on. 2D laminate nanomaterials demonstrate arguably better ultrathin film-forming ability through vacuum-assisted deposition techniques and offer a versatile platform for exploiting CO_2-philic or reactive molecules by incorporating them into the interlayer nanochannels.[41,133–135] Yet, defect control and reproducibility are immense challenges here too. Therefore, even though a number of these 2D or 3D nanostructure-based TFC membranes exhibited much better CO_2/N_2 performance than polymeric materials, especially in their CO_2 permeance which could reach a range of ~3000 to above 10 000 GPU with sufficient selectivities, their practicality has always been a question.[41,162,166,171,172]

To utilize the favorable gas transport characteristics of these nanostructures, mixed matrix membranes (MMMs) emerged as an effective and versatile composite material strategy by physically incorporating the nanoparticles as a dispersed filler phase into the continuous polymeric matrix. The incorporated nanofillers are expected to enhance the CO_2/N_2 separation in a number of ways, including (1) the provision of fast diffusion channels to enhance CO_2 permeance, (2) promoting more CO_2 preferential adsorption than N_2 to boost the selectivity, and (3) being simultaneously decorated with CO_2-philic or CO_2-reactive moieties, like PEO-based polymers, PVAm or ionic liquids, to offer additional performance enhancement.[23,80,153–155,157,158] Studies even found that the incorporation of 1D tube-like particles, like carbon nanotubes (CNTs), could effectively reduce the penetration of matrix polymers into the substrate pores, which is a very interesting area to explore for promoting two-layer TFC designs.[159] Again, unlike diffusivity–selectivity dominated separations, size selection is not a major enhancement factor exploited in CO_2/N_2-targeting MMMs. However, for MMMs, achieving uniform and finely sized filler dispersion remains a key challenge against their deployment in TFC membranes due to the inherent incompatibility between organic amorphous polymers and highly ordered nanostructures. This is especially a problem with 3D nanofillers, like 3D MOFs and zeolites, because the high self-crystalline/aggregation tendency and extended molecular architectures in these structures makes their size control very difficult and inconsistent, which have to be kept within a few tens of nanometers in order to be fully contained by an ultrathin polymeric film without protrusion or creating defects.[9] The requirement of high loading by 3D nanofillers (usually >30 wt%) also exacerbates this issue. In comparison, 2D anisotropic nanosheets, like GO, 2D MOFs or MXenes, are more MMM-friendly because their laminate structures with subnanoscale thickness and high aspect ratio allow an effective performance enhancement to be achieved at a tiny loading of even below 1 wt% which could better maintain the integrity of the ultrathin polymeric matrix.[52] Based on these observations, 2D zeolites or 2D zeolitic imidazole frameworks (ZIFs) could potentially be a promising filler choice because MFI-type zeolites show extraordinary CO_2/N_2 separation performance among inorganics and frameworks owing to their high CO_2 adsorption capacity and kinetics. 2D formation could reduce the loading and containment constraints for them.

Despite the many promises MMMs have brought, the heterogeneity between matrix and nanofillers, be it 2D or 3D, almost always poses the critical problem of nanodefect formation at the polymer–filler interface, which eventually makes consistent MMM production very difficult and costly.[196] Recent studies discovered that the incorporation of organic macrocyclic cavitands (OMCs), like calixarenes, with a small confined molecular structure and compatible solubility with matrix polymers could produce MMMs with perfect molecular homogeneity, also known as molecularly mixed composite membranes (MMCMs), which demonstrated significantly enhanced H_2/CO_2-sieving performance.[197,198] By completely retaining the polymeric nature in the resultant composite, the MMCMs show great potential for fabrication into thin films without encountering interfacial defects or other issues associated with phase segregation in traditional MMM designs.

6.3.6. Enhancing interfacial compatibility between the gutter and selective layers. Among all the existing TFC designs, PEO-based polymers are the most extensively researched selective layer materials because of their solution-compatibility with thin-film fabrication, ease of synthesis and functionalization, and outstanding CO_2/N_2 separation performance arising from the dipole–quadrupole interaction of their ethylene oxide units with CO_2.[199] However, interfacial compatibility between the PEO-based selective layer and PDMS gutter layer is an often-overlooked

discussion in most TFC studies. As the selective layer coating solution is made increasingly more dilute in the hope of obtaining a thinner layer, defects start to form, of which the minimum onset concentration is observed to depend on how easily wettable the PDMS surface is by the coating solution. That is, the interfacial interaction between the selective and gutter layers plays a critical role in thin-film formation. However, the hydrophobic nature of PDMS makes it poorly compatible with the hydrophilic PEO-based polymers and studies have reported difficulty in fabricating defect-free Pebax® thin-films on the PDMS gutter layer due to its inability to wet the PDMS surface well enough.[92,93,136] A number of post surface modification techniques have been explored to enhance the hydrophilicity and surface free energy of the PDMS gutter layer for better compatibilizing it with the selective layer, including polydopamine coating, surface plasma treatment, grafting of hydrophilic dendrimers and incorporating bifunctional aminosilanes.[36,200–202] However, the additional treatment step will invariably complicate the production and increase the burden for upscaling. In addition, these surface modifications through hydrophilic coating or surface functionalization often introduce extra transport resistance. Also, the plasma-induced surface hydrophilicity is not a permanent effect which attenuates with time and will cause storage issues in practical applications.

Instead of post-treatments, intrinsic material modification on either the gutter or selective layer could also be an effective method to reconcile their interfacial incompatibility. For example, like previously mentioned in the gutter layer section, PEO-based polymers or siloxane materials could be incorporated into PDMS *via* block copolymerization or physical mixing to increase its gutter layer hydrophilicity (water contact angle decreases significantly), which could promote better CO_2/N_2 separation performance by enhancing both the CO_2-philicity and interfacial compatibility.[128,129] This method could be slightly tuned and used as a hydrophilicity reduction strategy for the PEO-based selective layer too.

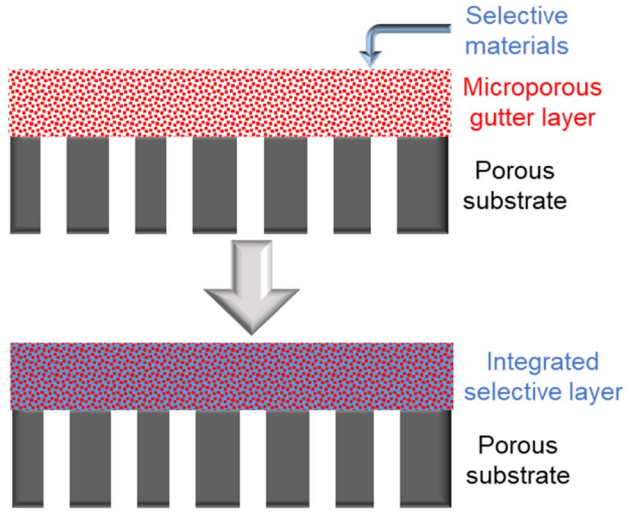

Fig. 8 Illustration of the proposed integrated-layer TFC design based on a microporous gutter layer.

Inspired by supported liquid membranes (SLMs) in which liquidous selective membrane materials are impregnated within microporous polymeric or inorganic supports by capillary forces, it is plausible and a bold idea to remove the concept of having a continuous smooth interface in TFC design by using a porous or sponge-like gutter layer that holds the selective layer materials within its pores to form an integrated layer as proposed in Fig. 8.[203] This way, surface compatibility becomes no longer an issue as it is now the capillary forces that keep everything in place rather than the interfacial interaction. Even liquidous selective materials, like small molecular weight PEO-based polymers or ionic liquids, could possibly be directly utilized in such an integrated layer design. Microporous polymers like PIMs or PTMSP are potential porous gutter layer candidates to explore.

Besides providing a more compatible and wettable surface for thin-film formation, the selective-gutter interface interaction could also impact the gas transport properties of the TFC membrane. Studies revealed a polymer chain interpenetration phenomenon at an oxygen plasma-treated Pebax®-PDMS interface due to the solvation and mixing of plasma-activated surface PDMS polymers in the Pebax® coating solution, which yielded a thin interpenetrated layer with better CO_2-philicity arising from its special molecular structure and chemistry.[136] Enhanced CO_2/N_2 selectivity was obtained from that. A similar phenomenon was found in the PIM-PTMSP interface too.[84] This interfacial interpenetration behavior, probably influenced by a combination of factors including solvent choice, polymer interaction, functionality, surface conditioning and more, could play a critical role in determining the overall TFC separation performance but is still very little understood. A mechanistic revelation is needed for advancing our knowledge of TFC interfacial chemistry.

6.3.7. Development of ultrathin-film fabrication techniques. Currently, direct surface coating methods, like dip coating or spray coating, are the most commonly used deposition techniques in TFC designs, which have also realized commercial applications. However, as mentioned before, defect-free ultrathin-film production using these conventional coating methods is very challenging, especially when the interfacial compatibility is poor. The few ultrathin film composite (UFC) membranes shown in Table 1 with a selective layer thickness in the range of 10^0–10^1 nm are largely produced by other better-controlled coating/deposition technologies, such as spin-coating, sacrificial transfer, vacuum-assisted filtration, or a combination of them. For example, the thinnest Pebax® layer (2–20 nm) and PDMS film (34 nm) were fabricated by well-controlled spin-coating on a sacrificial layer, followed by a careful secondary transfer onto the substrate.[88,136] The extreme delicacy involved in this strategy makes its practical large-scale application almost prohibitive. On the other hand, ultrathin-films of 2D laminate nanomaterials, like graphene and GO, could be obtained from vacuum filtration, which is a relatively more scalable technique but has a more restricted range of applicability (*i.e.* solid–liquid mixtures/suspensions).[41,134] In some rare cases, <100 nm defect-free films have been successfully fabricated by dip coating using high molecular weight polymers (*e.g.* PolyActive™ 4 K) while their low molecular weight

counterparts could not do the same.[54] This provides a key suggestion for desirable molecular properties in the selective materials other than their CO_2-affinity – molecular weight, which could be a design consideration for improving existing polymer-based materials. One emerging selective layer deposition method is called continuous assembly of polymers (CAP) which firstly deposits an initiator layer on top of the gutter layer, followed by atom transfer radical polymerization (ATRP) of the selective materials on top of the surface-initiated gutter layer into an ultrathin film.[130,140] The CAP technique goes well with MOF or MOF-containing surfaces because of their good affinity with the initiator. It presents a smooth combination of MOF-induced gutter layer enhancement with ultrathin selective layer production, which is a very promising deposition technology. Yet, the cost and scalability concerns of this multi-step reactive process are real.

6.3.8. Practical considerations for future materials development. In terms of CO_2/N_2 separation performance, quite a handful of existing state-of-the-art TFC materials developed in labs have greatly surpassed the new industrial targets that demand a CO_2 permeance of >3000 GPU and CO_2/N_2 selectivity of ~20–60. However, when we zoom out to take commercial developments into account, the separation performance realized by TFC membranes at the largest demonstrated scale (Gen 1 Polaris™) is still around the early industrial target level (~1000 GPU).[28,33] A few pilot-scale products could deliver better performance but are still far from the new cost-effective targets.[27,28,31] Apparently, there exists an enormous gap between bench-scale research and commercial TFC products that should warrant more research attention than it does now.

For instance, as we know that the separation performance generally tapers down as the scale upsizes, more simulation studies with practical models should be carried out to develop correlational understanding that could help extrapolate performance for larger scales and to also quantitatively reveal and assess potential critical performance-influencing factors. This could help develop translational knowledge which is currently very limited and constraining the scaling up of TFC membranes as established in Section 5.4.

Also, more research efforts in material development should be concurrently devoted to revitalizing existing designs with better upscaling potentials rather than just discovering new but less practical materials. This could be achieved by, for example, attempting larger-scale fabrication beyond the bench, developing better ultrathin coating techniques, optimizing the substrate pore structure, enhancing resistance against aging, plasticization and contaminants, or anything along these lines. Nevertheless, materials innovation is still a paramount goal for TFC research not merely because of the pursuit for better performance but also the constant refinement of design concepts and guidelines. In

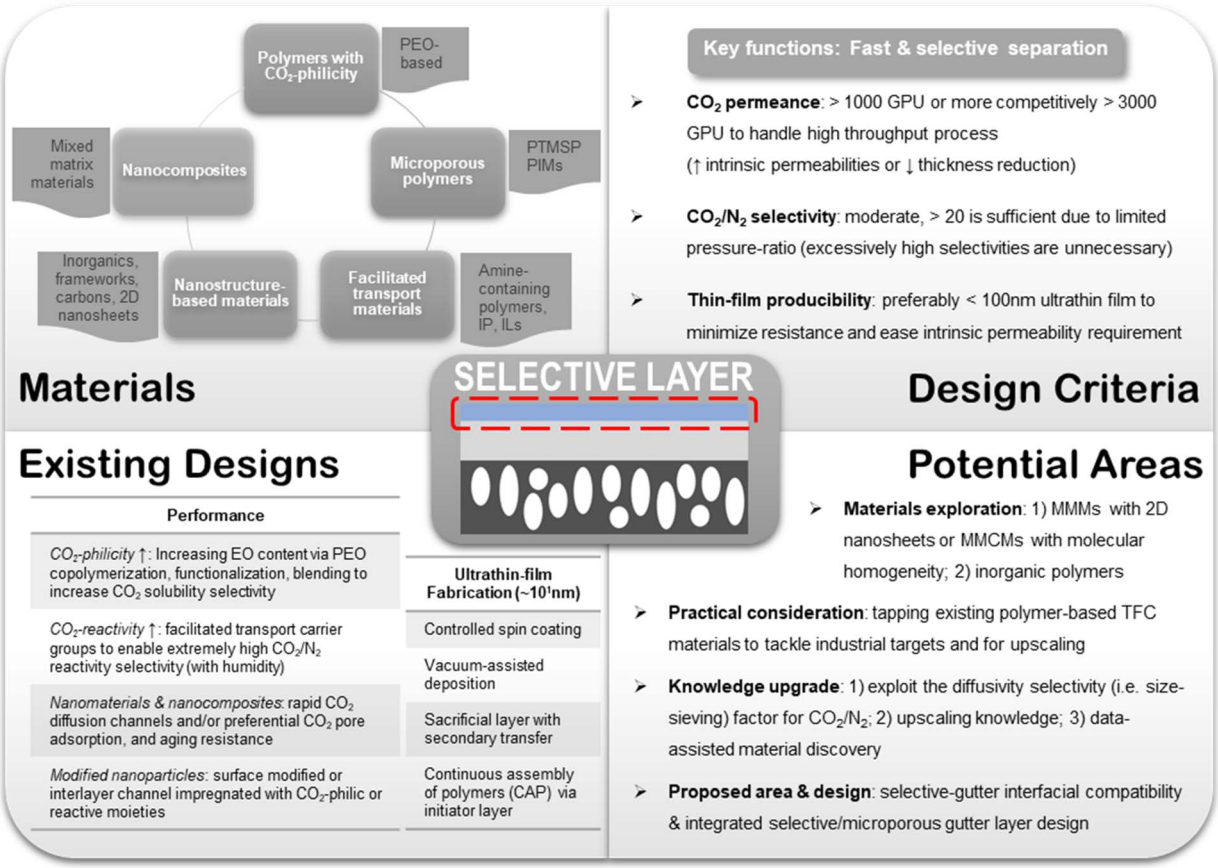

Fig. 9 Design summary for the selective layer.

light of this pursuit, data-assisted methods like machine learning (ML) could become an advantageous tool for the development of new TFC materials provided that more systematic structure–property relationship studies are conducted to afford better trained models. In fact, ML has already found numerous preliminary applications in membrane gas separation, such as predicting the performance of MOF-based MMMs or that of a number of different polymer building blocks, which are enabled through the large database available for these materials.[204–206] The many material-selection and design criteria discussed as well as the various potential research areas suggested in this entire section are summarized in Fig. 9.

7. From flat sheets to hollow fibers

7.1. Advantages of hollow fiber membranes

Hollow fiber membranes (HFMs) are a more industrially favored membrane configuration than flat sheet membranes (FSMs) because they offer much higher per volume membrane area than the latter, which allows the HFM modules to achieve up to 10 times higher packing density than the spiral-wound modules assembled from FSMs.[9,12,207] This packing efficiency will then translate into more compact equipment size and a smaller footprint that are in line with the design principles towards process intensification.[208] Most existing industrial membrane gas separations use asymmetric integrally skinned HFM modules for this reason.[11–13,67] However, for post-combustion CO_2 capture TFC membrane research, the majority of the lab studies and commercial developments revolve around the flat sheet configuration with very limited reports of TFC HFMs. PEEK-based TFC HFMs are to the best of our knowledge the only commercial HFM product reaching a pilot scale.[31] Although the essential idea of a layer-on-layer design remains the same in HFMs, the execution of each layer of coating is much more challenging on a vertical cylindrical geometry with a millimeter- or sub-millimeter size diameter. Firstly, obtaining a desirable surface pore structure on hollow fiber (HF) substrates requires strenuous optimization of the spinning conditions or the spinning line design which is arguably much more difficult and laborious than casting flat sheet (FS) substrates. Many trials-and-errors are involved in such a process because of the lack of systematic research and knowledge of the fabrication of TFC-applicable HF substrates and their eventual assembly into modules or the fact that the available knowledge usually remains as undisclosed trade-secrets.

7.2. Challenges in thin-film composite hollow fiber membrane fabrication

For TFC HFMs, the selective layer is generally applied *via* either dual-layer spinning or solution coating. The former allows the direct attachment of a thin selective layer onto the substrate *via* a co-extrusion process but is yet to be explored for TFC HFMs for CO_2/N_2 separation, to the best of our knowledge, presumably because of the stringent compatibility requirement in the choice of polymers and solvents to prevent detachment or defect formation.[209,210] It would be a potential area of interest for developing two-layer TFC HFMs because of its efficient one-step

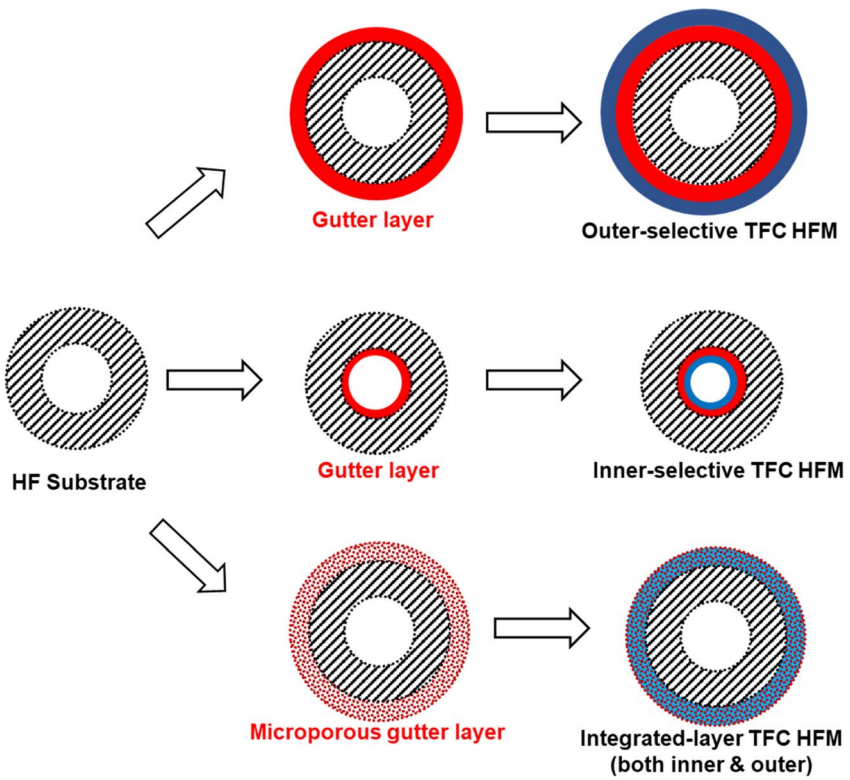

Fig. 10 Schematic illustration of the three possible TFC hollow fiber membrane structures.

production. As for surface coating methods, dip coating is most compatible with TFC HFMs while spray or spin coating is difficult or wasteful to be applied on fibers with small dimensions.[211] In a flat sheet configuration, the gravitational pull exerted on the dip-coated solution is perpendicular to the substrate surface and could be imagined as a natural "grip" for holding the solution on the flat surface which could aid its uniform spreading and curing. When it comes to hollow fibers, gravity is exerted longitudinally along the cylindrical surface in one direction and constantly pulling the solution down while it is curing, which makes the uniform deposition a much more challenging task than in flat sheets. This is especially an issue for three-layer TFC HFMs with a PDMS gutter layer because of the poor adhesion of hydrophilic polymer solution on the PDMS surface. Therefore, ensuring sufficient interfacial compatibility is of critical importance for HFM to obtain a uniform coating which could possibly be done *via* similar surface post-treatment or material modification strategies mentioned in the previous section.

7.3. Various hollow fiber membrane structures and their features

Generally, as shown by Fig. 10, TFC HFMs could be designed as being either inner-selective or outer-selective while the proposed integrated layer structure is also applicable in a fiber configuration as both the inner and outer layers. Outer-selective TFC HFMs require the coating process, usually dip coating, to be completed before being ready for module assembly which could pose handling issues at a large scale given the small dimensions and sheer number of fibers. Also, dip coating is a batch process which will demand carefully redesigned coating equipment and an optimized coating process in order to scale up the production. In comparison, inner-selective HFMs could be first assembled into modules before the coating solution is passed through the lumen side for continuous coating, which avoids the batch handling constraint and offers continuous production with less stringent equipment demand. However, the inner-selective coating solution needs to be judiciously formulated. If too viscous, the increased pumping force to push it through the narrow lumen could cause intrusion into the substrate pores. If too dilute, pore penetration could also occur, accompanied by possible defect formation. Another possible phenomenon to be observed with inner-selective HFMs is the pressure-dependence of their separation performance. At high operating pressures, a strong radially outward pressing force will be exerted on the inner wall of the fiber, causing deformation and circumferential straining of the selective, gutter and substrate skin layers, which could impact their separation performance as studies have shown strain-dependence of the gas transport properties of polymers. Besides the existing HFM structures, the proposed integrated layer design could be very advantageous for TFC HFMs because the selective materials could potentially be held within the porous gutter layer by the stronger capillary forces rather than relying on the interfacial interaction to fight against the downward pull.

7.4. Hollow fiber membranes *vs.* flat sheets

The CO_2/N_2 separation performance of a number of representative TFC HFMs is summarized in Fig. 11. Compared with the performance data shown previously in Fig. 4 obtained largely from flat sheets, TFC HFMs clearly show a less competitive

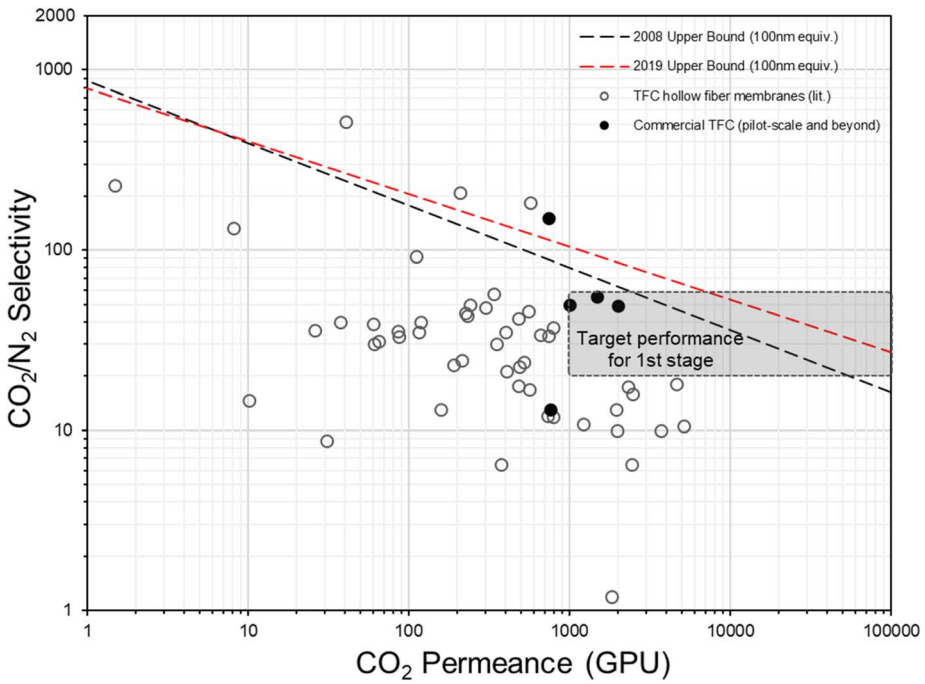

Fig. 11 Summary of the CO_2/N_2 separation performance of existing representative TFC hollow fiber membranes against the hypothesized thin-film upper bounds (assuming 100 nm thickness[9,21,28]) and proposed industrial targets.

range of performance which barely touches the early metrics of industrial interest. This is a reasonable observation given the tougher design constraints faced by HFMs. Therefore, more research on TFC HFM development should be conducted, in areas including but not limited to HF substrate optimization, coating process design, module assembly and interfacial modification, in order for this industrially favorable configuration to realize practical application for post-combustion CO_2 capture. Nevertheless, process advantages offered by HFMs would not make flat sheet membranes an inferior design. In fact, as mentioned before, commercial TFC membranes are mostly flat sheet spiral-wound modules which are also a very robust membrane configuration and a good platform for verifying many of the current state-of-the-art materials which are largely developed upon flat sheet substrates. Studies to transform FS designs into HFMs following such verifications would be a keen area for research that adds more practical value to TFC membranes.

8. Other perspectives

8.1 Discovery of a new class of materials and new separation mechanisms

Inorganic polymers with non-carbon-containing skeletons are a class of potential membrane materials that have rarely been explored for gas separation. Relatively recent studies have shown that blends of crosslinked polyphosphazene (PPZ) polymer, which is a phosphorus-skeleton inorganic polymer, could deliver both promising intrinsic and thin-film CO_2/N_2 separation performance.[152,212] These membranes also demonstrated outstanding stability against physical aging and humidity. Along with their great ease of post-synthesis functionalization that offers a highly expandable materials platform, these attractive traits in PPZ should bring more research attention to this new class of polymers. Another interesting area is to exploit the N_2/CO_2-selective materials to overcome the pressure-ratio-limitation. For example, it has been shown that the incorporation of certain transition metal ions like Fe^{3+} into the interlayer spacing of reduced GO membranes could allow a high N_2/CO_2 selectivity of over 90 to be achieved at a high N_2 permeance (>1000 GPU) owing to the extraordinary adsorption selectivity of Fe^{3+} for N_2 over CO_2.[213] The possibility to realize a similar reverse-selective mechanism in polymeric membranes will be an exciting subject for future exploration. In addition, polymerized ILs, like poly(ionene)s and poly(ionomer)s, with good solid film-forming ability could be a promising class of selective layer materials given the excellent intrinsic CO_2-affinity of many ILs.[214,215]

8.2 Performance under realistic conditions

Most existing performance tests were conducted using single gas or ideal gas mixtures with limited consideration of actual contaminants and composition variations. Simulated flue gas feed containing common contaminants present in actual flue gas, like SO_x and NO_x, should be used more in future studies. Performance and stability deterioration is almost unavoidable with real feed, which has to be critically assessed and countered. Investigation of the CO_2/O_2 separation properties of the TFC membranes is also very important given the presence of O_2 in the flue gas. Since the flue gas composition varies quite appreciably from place to place with a range of CO_2 concentrations, performance should be tested with varied feed composition to assess if there is any composition-dependence and to cater to the needs of different applications.

8.3 Transferability of TFC design to other gas separation

Reverse-selective CO_2/H_2 separation membranes targeting pre-combustion CO_2 capture from syngas are also dominated with the solubility-selective gas transport.[216,217] Therefore, many of the membrane materials with very high CO_2/N_2 selectivity, like PEO-based polymers and FTMs, show excellent CO_2/H_2 selectivity, which make them potential candidates for efficient membrane pre-combustion CO_2 capture.[218,219] However, the syngas streams are usually produced at high temperatures of >150 °C, which tends to reduce CO_2 solubility selectivity and increase diffusivity selectivity of the permeant, making the operating conditions unfavorable for CO_2/gas separation.[220] Also, most polymers do not possess the thermal stability to even withstand such kind of operating temperatures, making a pre-cooling step necessary for their implementation in this process. In addition, syngas typically has a high pressure of >10 bar which could induce significant plasticization. As for diffusivity–selectivity governed separations, the transferability of TFC materials is less likely. However, knowledge of substrate and gutter layer design as well as coating technology and thin-film production is all shareable, allowing the development of TFC technology in one application to benefit that in another.

8.4 Potential of TFC for direct air carbon capture (DACC)

Membrane capture is known to target point source emitters better, but their applicability for direct air capture, given their fast progress made in other CO_2 capture applications, has received more attention recently. In terms of process design, capturing CO_2 from air using membranes faces the same pressure-ratio limitation as post-combustion CO_2 capture with a much higher severity due to the extremely low CO_2 concentration of ~0.04% in air.[221] Only membranes with extremely high CO_2 permeances could be meaningful for this process, which to some extent aligns with the design criteria of a TFC gutter layer. Studies showed that ultrathin PDMS membranes (150 nm) with >10 000 GPU CO_2 permeance could achieve an appreciable CO_2 separation efficiency from a feed containing only 1000 ppm (0.1%) CO_2.[88] With the advancement in ultrathin-film fabrication and development of a multi-stage membrane separation unit, development of commercial DACC membranes may not be a completely impossible mission.

9. Conclusions

TFC membranes are a promising step undertaken by membrane researchers to progress from dense, thick materials to a configuration with high industrial potential. Despite the many

advantages TFC membranes offer, numerous design constraints are found in each of their constituting components from the substrate to the selective layer that have to be addressed concurrently because of their mutually influencing nature. These include the surface pore structure control for the substrate, pore intrusion and geometric restrictions by gutter or selective layers, defect-free ultrathin film production, interfacial interaction between layers of different surface compatibility, and scalable production and assembly. Strategies that could tackle one issue often result in a reduction in the scalable potential of the others. These challenges are hence the key technical barriers that hamper the translation of available TFC materials into large-scale membrane products. While the major forefront of current TFC research for post-combustion CO_2 capture falls in separation performance enhancement, it is highly recommended for more concerted research efforts to be dedicated to overcoming the technical and practical constraints delineated throughout this perspective, including but not limited to the development of scalable materials strategies to reduce aging, as well as more consistent porous substrate and ultrathin-film fabrication techniques, and obtaining systematic understanding of ultrathin-film state transport properties as well as translational knowledge and scale-up experience. In a nutshell, at the current stage, the most scalable TFC designs are still those based on polymers and hence a practical research area is to further refine the existing coating/deposition technology, improve interfacial compatibility and design new TFC configurations that could maximize the potential of currently available high-performance polymers. Discovery of new materials, on the other hand, should be less performance-driven but more towards the purpose of unraveling new materials concepts or structure–property relationships for guiding data-driven research approaches.

Conflicts of interest

There are no conflicts to declare.

Acknowledgements

The authors acknowledge the Low Carbon Energy Research Funding Initiative administrated by the Agency for Science, Technology and Research, Singapore under grant number A-8000182-00-00 for financial support.

Notes and references

1 International Energy Agency (IEA), *CO_2 Emissions in 2022*, IEA, Paris, 2023, **https://www.iea.org/reports/co2-emissions-in-2022**, (accessed 12 April 2023).
2 *Carbon Dioxide Emissions From Electricity*, World Nuclear Association, **https://www.world-nuclear.org/information-library/energy-and-the-environment/carbon-dioxide-emissions-from-electricity.aspx**, (accessed 12 April 2023).
3 Q. Lin, X. Zhang, T. Wang, C. Zheng and X. Gao, *Engineering*, 2022, **14**, 27–32.
4 M. Bui, C. S. . Adjiman, A. Bardow, E. J. Anthony, A. Boston, S. Brown, P. S. Fennell, S. Fuss, A. Galindo, L. A. Hackett, J. P. Hallett, H. J. Herzog, G. Jackson, J. Kemper, S. Krevor, G. C. Maitland, M. Matuszewski, I. S. Metcalfe, C. Petit, G. Puxty, J. Reimer, D. M. Reiner, E. S. Rubin, S. A. Scott, N. Shah, B. Smit, J. P. M. Trusler, P. Webley, J. Wilcox and N. M. Dowell, *Energy Environ. Sci.*, 2018, **11**, 1062–1176.
5 T. Fout, A. Zoelle, D. Keairns, M. Turner, M. Woods, N. Kuehn, V. Shah, V. Chou and L. Pinkerton, *Cost and Performance Baseline for Fossil Energy Plants Volume 1a: Bituminous Coal (PC) and Natural Gas to Electricity Revision 3*, Report Number: DOE/NETL-2015/1723, U.S. Department of Energy, Washington, DC, USA, 2015.
6 T. C. Merkel, X. Wei, Z. He, L. S. White, J. G. Wijmans and R. W. Baker, *Ind. Eng. Chem. Res.*, 2013, **52**, 1150–1159.
7 T. C. Merkel, H. Lin, X. Wei and R. Baker, *J. Membr. Sci.*, 2010, **359**, 126–139.
8 D. S. Sholl and R. P. Lively, *Nature*, 2016, **532**, 435–437.
9 M. Liu, M. D. Nothling, S. Zhang, Q. Fu and G. G. Qiao, *Prog. Polym. Sci.*, 2022, **126**, 101504.
10 A. F. Ismail, K. C. Khulbe and T. Matsuura, in *Gas Separation Membranes: Polymeric and Inorganic*, Springer International Publishing, Cham, 2015, pp. 11–35.
11 R. Prasad, F. Notaro and D. R. Thompson, *J. Membr. Sci.*, 1994, **94**, 225–248.
12 R. W. Baker, *Membrane Technology and Applications*, John Wiley & Sons Ltd, United Kingdom, 3rd edn, 2012.
13 R. W. Baker and K. Lokhandwala, *Ind. Eng. Chem. Res.*, 2008, **47**, 2109–2121.
14 R. W. Baker, Future directions of membrane gas separation technology, *Ind. Eng. Chem. Res.*, 2002, **41**, 1393–1411.
15 J. Wu, S. Japip and T. S. Chung, *Mater. Res. Found.*, 2021, **113**, 243–334.
16 Y. Han and W. S. W. Ho, *J. Polym. Eng.*, 2020, **40**, 529–542.
17 V. I. Bondar, B. D. Freeman and I. Pinnau, *J. Polym. Sci., Part B: Polym. Phys.*, 2000, **38**, 2051–2062.
18 Y. Han and W. S. W. Ho, *J. Membr. Sci.*, 2021, **628**, 119244.
19 T. C. Merkel, V. I. Bondar, K. Nagai, B. D. Freeman and I. Pinnau, *J. Polym. Sci., Part B: Polym. Phys.*, 2000, **38**, 415–434.
20 M. Liu, M. D. Nothling, P. A. Webley, Q. Fu and G. G. Qiao, *Acc. Chem. Res.*, 2019, **52**, 1905–1914.
21 B. Comesaña-Gándara, J. Chen, C. G. Bezzu, M. Carta, I. Rose, M.-C. Ferrari, E. Esposito, A. Fuoco, J. C. Jansen and N. B. McKeown, *Energy Environ. Sci.*, 2019, **12**, 2733–2740.
22 K. Nagai, T. Masuda, T. Nakagawa, B. D. Freeman and I. Pinnau, Poly[1-(trimethylsilyl)-1-propyne] and related polymers: synthesis, properties and functions, *Prog. Polym. Sci.*, 2001, **26**, 721–798.
23 M. J. Yoo, K. H. Kim, J. H. Lee, T. W. Kim, C. W. Chung, Y. H. Cho and H. B. Park, *J. Membr. Sci.*, 2018, **566**, 336–345.
24 C. Z. Liang, T.-S. Chung and J.-Y. Lai, *Prog. Polym. Sci.*, 2019, **97**, 101141.
25 M. Galizia, W. S. Chi, Z. P. Smith, T. C. Merkel, R. W. Baker and B. D. Freeman, *Macromolecules*, 2017, **50**, 7809–7843.

26 B. W. Rowe, B. D. Freeman and D. R. Paul, *Polymer*, 2009, **50**, 5565–5575.
27 T. Brinkmann, J. Lillepärg, H. Notzke, J. Pohlmann, S. Shishatskiy, J. Wind and T. Wolff, *Engineering*, 2017, **3**, 485–493.
28 L. S. Whitea, K. D. Amo, T. Wu and T. C. Merkel, *J. Membr. Sci.*, 2017, **542**, 217–225.
29 Membrane Technology and Research Inc., Scale-Up and Testing of Advanced Polaris Membrane CO2 Capture Technology (FE0031591), *2019 NETL CCUSOG Integrated Review Meeting*, 2019, **https://netl.doe.gov/node/9041**, (accessed 13 May 2023).
30 V. Vakharia, W. Salim, D. Wu, Y. Han, Y. Chen, L. Zhao and W. S. W. Ho, *J. Membr. Sci.*, 2018, **555**, 379–387.
31 S. Lia, T. J. Pyrzynski, N. B. Klinghoffer, T. Tamale, Y. Zhong, J. L. Aderhold, S. J. Zhou, H. S. Meyer, Y. Ding and B. Bikson, *J. Membr. Sci.*, 2017, **527**, 92–101.
32 C. A. Scholes, A. Qader, G. W. Stevens and S. E. Kentish, *Greenhouse Gases: Sci. Technol.*, 2015, **5**, 229–237.
33 US Department of Energy, *DOE Awards Approximately $99 Million for Demonstration of Large-Scale Pilot Carbon Capture Technologies*, Office of Fossil Energy and Carbon Management, 2021, **https://www.Energy.Gov/fe/articles/doe-awards-approximately-99-million-demonstration-large-scale-pilot-carbon-capture**, (accessed 13 May 2023).
34 L. M. Robeson, *J. Membr. Sci.*, 2008, **320**, 390–400.
35 L. M. Robeson, *J. Membr. Sci.*, 1991, **62**, 165–185.
36 Y. Wang, X. Ma, B. S. Ghanem, F. Alghunaimi, I. Pinnau and Y. Han, *Mater. Today Nano*, 2018, **3**, 69–95.
37 K. Kusakabe, T. Kuroda, A. Murata and S. Morooka, *Ind. Eng. Chem. Res.*, 1997, **36**, 649–655.
38 G. Xomeritakis, C. Y. Tsai and C. J. Brinker, *Sep. Purif. Technol.*, 2005, **42**, 249–257.
39 D. J. Babu, G. He, J. Hao, M. T. Vahdat, P. A. Schouwink, M. Mensi and K. V. Agrawal, *Adv. Mater.*, 2019, **3**, 1900855.
40 Y. Ying, Z. Yang, D. Shi, S. B. Peh, Y. Wang, X. Yu, H. Yang, K. Chai and D. Zhao, *J. Membr. Sci.*, 2021, **632**, 119384.
41 G. He, S. Huang, L. F. Villalobos, J. Zhao, M. Mensi, E. Oveisi, M. Rezaeia and K. V. Agrawal, *Energy Environ. Sci.*, 2019, **12**, 3305–3312.
42 H. W. Kim, H. W. Yoon, S. M. Yoon, B. M. Yoo, B. K. Ahn, Y. H. Cho, H. J. Shin, H. Yang, U. Paik, S. Kwon, J. Y. Choi and H. B. Park, *Science*, 2013, **342**, 91–95.
43 J. Deng, J. Yu, Z. Dai and L. Deng, *Ind. Eng. Chem. Res.*, 2019, **58**, 5261–5268.
44 Y. Chen and W. S. W. Ho, *J. Membr. Sci.*, 2016, **514**, 376–384.
45 Y. Cheng, Y. Ying, S. Japip, S. D. Jiang, T. S. Chung, S. Zhang and D. Zhao, *Adv. Mater.*, 2018, **30**, 1802401.
46 C. Z. Liang, W. F. Yong and T.-S. Chung, *J. Membr. Sci.*, 2017, **541**, 367–377.
47 X. Jiang, K. Goh and R. Wang, *J. Membr. Sci.*, 2022, **658**, 120741.
48 P. Li, Z. Wang, W. Li, Y. Liu, J. Wang and S. Wang, *ACS Appl. Mater. Interfaces*, 2015, **7**, 15481–15493.
49 R. S. Bhavsara, T. Mitrab, D. J. Adams, A. I. Cooper and P. M. Budd, *J. Membr. Sci.*, 2018, **564**, 878–886.
50 Y. Huang, T. C. Merkel and R. W. Baker, *J. Membr. Sci.*, 2014, **463**, 33–40.
51 J. Xu, Z. Wang, Z. Qiao, H. Wu, S. Dong, S. Zhao and J. Wang, *J. Membr. Sci.*, 2019, **581**, 195–213.
52 H. B. Park, J. Kamcev, L. M. Robeson, M. Elimelech and B. D. Freeman, *Science*, 2017, **356**, eaab0530.
53 H. Guo, W. Xu, J. Wei, Y. Ma, Z. Qin, Z. Dai, J. Deng and L. Deng, *Membranes*, 2023, **13**, 359.
54 W. Yave, A. Car, J. Wind and K.-V. Peinemann, *Nanotechnology*, 2010, **21**, 395301.
55 T.-J. Kim, H. Vralstad, M. Sandru and M.-B. Hagg, *J. Membr. Sci.*, 2013, **428**, 218–224.
56 Y. Chen, B. Wang, L. Zhao, P. Dutta and W. S. W. Ho, *J. Membr. Sci.*, 2015, **495**, 415–423.
57 H. Lin and B. D. Freeman, *J. Mol. Struct.*, 2005, **739**, 57–74.
58 Y. Shi, C. M. Burns and X. Feng, *J. Mol. Struct.*, 2006, **282**, 115–123.
59 E. Favre, *J. Membr. Sci.*, 2007, **294**, 50–59.
60 M. Ai, S. Shishatskiy, J. Wind, X. Zhang, C. T. Nottbohm, N. Mellech, A. Winter, H. Vieker, J. Qiu, K.-J. Dietz, A. Gölzhäuser and A. Beyer, *Adv. Mater.*, 2014, **26**, 3421–3426.
61 J. M. S. Henis and M. K. Tripodi, *J. Membr. Sci.*, 1981, **8**, 233–246.
62 A. Fouda, Y. Chen, J. Bai and T. Matsuura, *J. Membr. Sci.*, 1991, **64**, 263–271.
63 N. Itoh, T.-H. Wu and K. Haraya, *J. Membr. Sci.*, 1995, **99**, 175–183.
64 K. A. Lundy and I. Cabasso, *Ind. Eng. Chem. Res.*, 1989, **28**, 742–756.
65 T.-S. Chung, *Sep. Purif. Technol.*, 1997, **12**, 17–23.
66 S. Loeb and S. Sourirajan, in *Saline Water Conversion—II*, ed. R. F. Gould, American Chemical Society, Washington, D.C., 1963, pp. 117–132.
67 J. M. S. Henis and M. K. Tripodi, Multicomponent membranes for gas separations, *US Pat.*4230463A, 1980.
68 W. J. Schell and C. D. Houston, Spiral-wound permeators for purifications and recovery, *Chem. Eng. Prog.*, 1982, **78**, 33–37.
69 B. Zornoza, C. Casado and A. Navajas, in *Renewable Hydrogen Technologies*, ed. L. M. Gandía, G. Arzamendi and P. M. Diéguez, Elsevier, Amsterdam, 2013, pp. 245–268.
70 R. W. Baker and B. T. Low, *Macromolecules*, 2014, **47**, 6999–7013.
71 H. Makino, Y. Kusuki, H. Yoshida and A. Nakamaura, Process for preparing aromatic polyimide semipermeable membranes, *US Pat.*, 4378324, 1983.
72 J.-Y. Lai, M.-J. Liu and K.-R. Lee, *J. Membr. Sci.*, 1994, **86**, 103–118.
73 M. Pourafshari Chenar, M. Soltanieh, T. Matsuura, A. Tabe-Mohammadib and C. Feng, *Sep. Purif. Technol.*, 2006, **51**, 359–366.
74 Y. Medina-Gonzalez, E. Lasseuguette, J.-C. Rouch and J.-C. Remigy, *Sep. Sci. Technol.*, 2012, **47**, 1596–1605.
75 P. Ji, Y. Cao, X. Jie, M. Li and Q. Yuan, *Sep. Purif. Technol.*, 2010, **71**, 160–167.

76 X. Jiang, C. Y. Chuah, K. Goh and R. Wang, *J. Membr. Sci.*, 2021, **638**, 119708.
77 R. Vendamme, S.-Y. Onoue, A. Nakao and T. Kunitake, *Nat. Mater.*, 2006, **5**, 494–501.
78 M. Liu, P. A. Gurr, Q. Fu, P. A. Webley and G. G. Qiao, *J. Mater. Chem. A*, 2018, **6**, 23169–23196.
79 M. Kanezashi, J. O'Brien-Abraham, Y. S. Lin and K. Suzuki, *AIChE J.*, 2008, **54**, 1478–1486.
80 K. Xiea, Q. Fu, J. Kim, H. Lu, Y. He, Q. Zhao, J. Scofield, P. A. Webley and G. G. Qiao, *J. Membr. Sci.*, 2017, **535**, 350–356.
81 R. Semino, J. C. Moreton, N. A. Ramsahye, S. M. Cohen and G. Maurin, *Chem. Sci.*, 2018, **9**, 315–324.
82 M. Kattula, K. Ponnuru, L. Zhu, W. Jia, H. Lin and E. P. Furlani, *Sci. Rep.*, 2015, **5**, 15016.
83 S. D. Bazhenov, I. L. Borisov, D. S. Bakhtin, A. N. Rybakova, V. S. Khotimskiy, S. P. Molchanov and V. V. Volkov, *Green Energy Environ.*, 2016, **1**, 235e245.
84 I. Borisov, D. Bakhtin, J. M. Luque-Alled, A. Rybakova, V. Makarova, A. B. Foster, W. J. Harrison, V. Volkov, V. Polevaya, P. Gorgojo, E. Prestat, P. M. Budd and A. Volkov, *J. Mater. Chem. A*, 2019, **7**, 6417–6430.
85 M. Liu, M. D. Nothling, P. A. Webley, J. Jin, Q. Fu and G. G. Qiao, *Chem. Eng. J.*, 2020, **396**, 125328.
86 J. Wu, S. Japip and T.-S. Chung, *J. Mater. Chem. A*, 2020, **8**, 6196–6209.
87 L. Zhu, V. A. Kusuma, D. Hopkinson, K. P. Resnik and Z. Tong, Highly permeable supported pdms ultrathin films as a gutter layer for gas separation composite membranes, *2020 Virtual AIChE Annual Meeting*, 2020, **https://www.aiche.org/academy/conferences/aiche-annual-meeting/2020/proceeding/paper/343h-highly-permeable-supported-pdms-ultrathin-films-gutter-layer-gas-separation-composite-membranes**, (accessed 15 Apr 2023).
88 S. Fujikawa, M. Ariyoshi, R. Selyanchyn and T. Kunitake, *Chem. Lett.*, 2019, **48**, 1351–1354.
89 G. Firpo, E. Angeli, L. Repetto and U. Valbusa, *J. Membr. Sci.*, 2015, **481**, 1–8.
90 M. A. Islam and H. Buschatz, *Indian J. Chem. Technol.*, 2005, **12**, 88–92.
91 G. Zhang, T. N. Tran, L. Huang, E. Deng, A. Blevins, W. Guo, Y. Ding and H. Lin, *J. Membr. Sci.*, 2022, **644**, 120184.
92 X. Ren, J. Ren, H. Li, S. Feng and M. Deng, *Int. J. Greenhouse Gas Control*, 2012, **8**, 111–120.
93 L. Wang, Y. Lia, S. Li, P. Ji and C. Jiang, *J. Energy Chem.*, 2014, **23**, 717–725.
94 H. Z. Chen, Z. Thong, P. Li and T.-S. Chung, *Int. J. Hydrogen Energy*, 2014, **39**, 5043–5053.
95 P. Li, H. Z. Chen and T.-S. Chung, *J. Membr. Sci.*, 2013, **434**, 18–25.
96 F.-J. Tsai, D. Kang and M. Anand, *Sep. Sci. Technol.*, 1995, **30**, 1639–1652.
97 S. A. Stern, *J. Membr. Sci.*, 1994, **94**, 1–65.
98 C. E. Powell and G. G. Qiao, *J. Membr. Sci.*, 2006, **279**, 1–49.
99 J. C. White, P. K. Dutta, K. Shqau and H. Verweij, *Langmuir*, 2010, **26**, 10287–10293.
100 C. Wang, R. Shao, G. Wang, J. Zhao, Z. Sha and S. Sun, *Surf. Coat. Technol.*, 2021, **412**, 127016.
101 R. Gloukhovski, V. Freger and Y. Tsur, *Rev. Chem. Eng.*, 2018, **34**, 455–479.
102 X. Zhao, G. Meng, Q. Xu, F. Han and Q. Huang, *Adv. Mater.*, 2010, **22**, 2637–2641.
103 M. F. Twibi, M. H. D. Othman, S. K. Hubadillah, S. A. Alftessi, T. A. Kurniawan, A. F. Ismail, M. A. Rahman, J. Jaafar and Y. O. Raji, *Ceram. Int.*, 2021, **47**, 15367–15382.
104 X. Lia, Q. Lia, W. Fang, R. Wang and W. B. Krantz, *J. Membr. Sci.*, 2019, **580**, 12–23.
105 L. Liu, N. Jiang, C. M. Burns, A. Chakma and X. Feng, *J. Membr. Sci.*, 2009, **338**, 153–160.
106 R. Wang and T.-S. Chung, *J. Membr. Sci.*, 2001, **188**, 29–37.
107 X. M. Tan and D. Rodrigue, *Polymers*, 2019, **11**, 1160.
108 M. Khorsand-Ghayeni, J. Barzin, M. Zandi and M. Kowsari, *Polym. Bull.*, 2017, **74**, 2081–2097.
109 U. Beuscher and C. H. Gooding, *J. Membr. Sci.*, 1997, **132**, 213–227.
110 M. Shi, C. Dong, Z. Wang, X. Tian, S. Zhao and J. Wang, *Chin. J. Chem. Eng.*, 2019, **27**, 1807–1816.
111 D.-M. Wang and J.-Y. Lai, *Curr. Opin. Chem. Eng.*, 2013, **2**, 229–237.
112 G. R. Guillen, Y. Pan, M. Li and E. M. V. Hoek, *Ind. Eng. Chem. Res.*, 2011, **50**, 3798–3817.
113 C.-Y. Yang, G.-D. Zhu, Z. Yi, Y. Zhou and C.-J. Gao, *Chem. Eng. J.*, 2021, **424**, 128912.
114 K.-V. Peinemann, V. Abetz and P. F. W. Simon, *Nat. Mater.*, 2007, **6**, 992–996.
115 S. K. Elsaidi, M. Ostwal, L. Zhu, A. Sekizkardes, M. H. Mohamed, M. Gipple, J. R. McCutcheon and D. Hopkinsona, *RSC Adv.*, 2021, **11**, 25658–25663.
116 M. R. Chowdhury, J. Steffes, B. D. Huey and J. R. McCutcheon, *Science*, 2018, **361**, 682–686.
117 B. G. Thiam, A. E. Magri, H. R. Vanaei and S. Vaudreuil, *Polymers*, 2022, **14**, 1023.
118 F. Zhang, Y. Ma, J. Liao, V. Breedveld and R. P. Lively, *Macromol. Rapid Commun.*, 2018, **39**, 1800274.
119 T.-S. Chung, E. R. Kafchinski, R. S. Kohn, P. Foley and R. S. Straff, *J. Appl. Polym. Sci.*, 1994, **53**, 701–708.
120 I. Blume and I. Pinnau, Composite membrane, method of preparation and use, *US Pat.*4,963,165, 1990.
121 C. Z. Liang, J. T. Liu, J.-Y. Lai and T.-S. Chung, *J. Membr. Sci.*, 2018, **563**, 93–106.
122 S. Ohyabu, S. Kawai, T. Okamoto and T. Migaki, Composite hollow fiber-type separation membranes, processes for the preparation thereof and their use, *US Pat.*4664669, 1987.
123 M. E. Rezac and W. J. Koros, *J. Appl. Polym. Sci.*, 1992, **46**, 1927–1938.
124 T. Masuda, Y. Iguchi, B.-Z. Tang and T. Higashimura, *Polymer*, 1988, **29**, 2041–2049.
125 L. M. Robeson, W. F. Burgoyne, M. Langsam, A. C. Savoca and C. F. Tien, *Polymer*, 1994, **35**, 4970–4978.
126 D. S. Bakhtin, L. A. Kulikov, S. A. Legkov, V. S. Khotimskiy, I. S. Levin, I. L. Borisov, A. L. Maksimov, V. V. Volkov,

E. A. Karakhanov and A. V. Volkov, *J. Membr. Sci.*, 2018, **554**, 211–220.
127 L. Olivieri, S. Meneguzzo, S. Ligi, A. Saccani, L. Giorgini, A. Orsini, A. Pettinau and M. G. D. Angelis, *J. Membr. Sci.*, 2018, **555**, 258–267.
128 J. M. P. Scofield, P. A. Gurr, J. Kim, Q. Fu, A. Halim, S. E. Kentish and G. G. Qiao, *J. Polym. Sci., Part A: Polym. Chem.*, 2015, **53**, 1500–1511.
129 Y. Ji, M. Zhang, K. Guan, J. Zhao, G. Liu and W. Jin, *Adv. Funct. Mater.*, 2019, **29**, 1900735.
130 M. Liu, K. Xie, M. D. Nothling, L. Zu, S. Zhao, D. J. E. Harvie, Q. Fu, P. A. Webley and G. G. Qiao, *ACS Cent. Sci.*, 2021, **7**, 671–680.
131 J. Liu, Y. Pan, J. Xu, Z. Wang, H. Zhu, G. Liu, J. Zhong and W. Jin, *J. Membr. Sci.*, 2023, **667**, 121183.
132 M. Liu, K. Xie, M. D. Nothling, P. A. Gurr, S. S. L. Tan, Q. Fu, P. A. Webley and G. G. Qiao, *ACS Nano*, 2018, **12**, 11591–11599.
133 W. Ying, J. Cai, K. Zhou, D. Chen, Y. Ying, Y. Guo, X. Kong, Z. Xu and X. Peng, *ACS Nano*, 2018, **12**, 5385–5393.
134 F. Zhou, H. N. Tien, W. L. Xu, J.-T. Chen, Q. Liu, E. Hicks, M. Fathizadeh, S. Li and M. Yu, *Nat. Commun.*, 2017, **8**, 2107.
135 F. Zhou, H. N. Tien, Q. Dong, W. L. Xu, H. Li, S. Li and M. Yu, *J. Membr. Sci.*, 2019, **573**, 184–191.
136 O. Selyanchyn, R. Selyanchyn and S. Fujikawa, *ACS Appl. Mater. Interfaces*, 2020, **12**, 33196–33209.
137 J. H. Kim, S. Y. Ha and Y. M. Lee, *J. Membr. Sci.*, 2001, **190**, 179–193.
138 W. Yave, A. Car, S. S. Funari, S. P. Nunes and K.-V. Peinemann, *Macromolecules*, 2010, **43**, 326–333.
139 A. Halim, Q. Fu, Q. Yong, P. A. Gurr, S. E. Kentish and G. G. Qiao, *J. Mater. Chem. A*, 2014, **2**, 4999–5009.
140 K. Xie, Q. Fu, C. Xu, H. Lu, Q. Zhao, R. Curtain, D. Gu, P. A. Webley and G. G. Qiao, *Energy Environ. Sci.*, 2018, **11**, 544–550.
141 X. Ding, M. M. Hua, H. Zhao, P. Yang, X. Chen, Q. Xin and Y. Zhang, *J. Membr. Sci.*, 2017, **531**, 129–137.
142 Y. Wang, T. Hu, H. Li, G. Dong, W. Wong and V. Chen, *Energy Procedia*, 2014, **63**, 202–209.
143 J. M. P. Scofield, P. A. Gurr, J. Kim, Q. Fu, S. E. Kentish and G. G. Qiao, *J. Membr. Sci.*, 2016, **499**, 191–200.
144 Q. Fu, E. H. H. Wong, J. Kim, J. M. P. Scofield, P. A. Gurr, S. E. Kentish and G. G. Qiao, *J. Mater. Chem. A*, 2014, **2**, 17751–17756.
145 X. Yu, Z. Wang, Z. Wei, S. Yuan, J. Zhao, J. Wang and S. Wang, *J. Membr. Sci.*, 2010, **362**, 265–278.
146 S. Li, Z. Wang, C. Zhang, M. Wang, F. Yuan, J. Wang and S. Wang, *J. Membr. Sci.*, 2013, **436**, 121–131.
147 S. Li, Z. Wang, X. Yu, J. Wang and S. Wang, *Adv. Mater.*, 2012, **24**, 3196–3200.
148 M. Wang, Z. Wang, S. Li, C. Zhang, J. Wang and S. Wang, *Energy Environ. Sci.*, 2013, **6**, 539–551.
149 L. Deng, T.-J. Kim and M.-B. Hägg, *J. Membr. Sci.*, 2009, **340**, 154–163.
150 Y. Chen, L. Zhao, B. Wang, P. Dutta and W. S. W. Ho, *J. Membr. Sci.*, 2016, **497**, 21–28.
151 Z. Qiao, S. Zhao, M. Sheng, J. Wang, S. Wang, Z. Wang, C. Zhong and M. D. Guiver, *Nat. Mater.*, 2019, **18**, 163–168.
152 V. A. Kusuma, J. S. McNally, J. S. Baker, Z. Tong, L. Zhu, C. J. Orme, F. F. Stewart and D. P. Hopkinson, *ACS Appl. Mater. Interfaces*, 2020, **12**, 30787–30795.
153 J. Kim, Q. Fu, K. Xie, J. M. P. Scofield, S. E. Kentish and G. G. Qiao, *J. Membr. Sci.*, 2016, **515**, 54–62.
154 K. Xie, Q. Fu, P. A. Webley and G. G. Qiao, *Angew. Chem., Int. Ed.*, 2018, **57**, 8597–8602.
155 J. Kim, Q. Fu, J. M. P. Scofield, S. E. Kentish and G. G. Qiao, *Nanoscale*, 2016, **8**, 8312–8323.
156 R. Xu, Z. Wang, M. Wang, Z. Qiao and J. Wang, *J. Membr. Sci.*, 2019, **573**, 455–464.
157 B. Wang, Z. Qiao, J. Xu, J. Wang, X. Liu, S. Zhao, Z. Wang and M. D. Guiver, *Adv. Mater.*, 2020, **32**, 1907701.
158 Y. Yuan, Z. Qiao, J. Xu, J. Wang, S. Zhao, X. Cao, Z. Wang and M. D. Guiver, *J. Membr. Sci.*, 2021, **620**, 118923.
159 Y. Han, D. Wu and W. S. W. Ho, *J. Membr. Sci.*, 2018, **567**, 261–271.
160 Y. Wang, H. Jin, Q. Ma, K. Mo, H. Mao, A. Feldhoff, X. Cao, Y. Li, F. Pan and Z. Jiang, *Angew. Chem., Int. Ed.*, 2020, **59**, 4365–4369.
161 P. Nian, Y. Li, X. Zhang, Y. Cao, H. Liu and X. Zhang, *ACS Appl. Mater. Interfaces*, 2018, **10**, 4151–4160.
162 C. Yu, Y. Liang, W. Xue, Z. Zhang, X. Jia, H. Huang, Z. Qiao, D. Mei and C. Zhong, *J. Membr. Sci.*, 2021, **625**, 119139.
163 R. Rong, Y. Sun, T. Ji and Y. Liu, *J. Membr. Sci.*, 2020, **610**, 118275.
164 W. Wu, Z. Li, Y. Chen and W. Li, *Environ. Sci. Technol.*, 2019, **53**, 3764–3772.
165 Z. Zhao, X. Ma, A. Kasik, Z. Li and Y. S. Lin, *Ind. Eng. Chem. Res.*, 2013, **52**, 1102–1108.
166 H. Yin, J. Wang, Z. Xie, J. Yang, J. Bai, J. Lu, Y. Zhang, D. Yin and J. Y. S. Lin, *Chem. Commun.*, 2014, **50**, 3699–3701.
167 Y. Ying, Z. Zhang, S. B. Peh, A. Karmakar, Y. Cheng, J. Zhang, L. Xi, C. Boothroyd, Y. M. Lam, C. Zhong and D. Zhao, *Angew. Chem.*, 2021, **133**, 11419–11426.
168 M. P. Bernal, J. Coronas, M. Menendez and J. Santamaria, *AIChE J.*, 2004, **50**, 127–135.
169 Y. Hasegawa, K. Watanabe, K. Kusakabe and S. Morooka, *Sep. Purif. Technol.*, 2001, **22–23**, 319–325.
170 H. Guo, G. Zhu, H. Li, X. Zou, X. Yin, W. Yang, S. Qiu and R. Xu, *Angew. Chem., Int. Ed.*, 2006, **45**, 7053–7056.
171 S. Li and C. Q. Fan, *Ind. Eng. Chem. Res.*, 2010, **49**, 4399–4404.
172 K. Kusakabe, T. Kuroda and S. Morooka, *J. Membr. Sci.*, 1998, **148**, 12–23.
173 C.-Y. Tsai, S.-Y. Tam, Y. Lu and C. J. Brinker, *J. Membr. Sci.*, 2000, **169**, 255–268.
174 S. Zhang, H. Li, H. Li, B. Sengupta, S. Zha, S. Li and M. Yu, *Adv. Funct. Mater.*, 2020, **30**, 2002804.
175 Q. Song, S. Cao, R. H. Pritchard, B. Ghalei, S. A. Al-Muhtaseb, E. M. Terentjev, A. K. Cheetham and E. Sivaniah, *Nat. Commun.*, 2014, **5**, 4813.
176 H. B. Park, C. H. Jung, Y. M. Lee, A. J. Hill, S. J. Pas, S. T. Mudie, E. V. Wagner, B. D. Freeman and D. J. Cookson, *Science*, 2007, **318**, 254–258.

177 P. S. Tin, T.-S. Chung, Y. Liu and R. Wang, *Carbon*, 2004, **42**, 3123–3131.
178 S. Kim, S. H. Han and Y. M. Lee, *J. Membr. Sci.*, 2012, **403–404**, 169–178.
179 K. T. Woo, J. Lee, G. Dong, J. S. Kim, Y. S. Do, W.-S. Hung, K.-R. Lee, G. Barbieri, E. Drioli and Y. M. Lee, *J. Membr. Sci.*, 2015, **490**, 129–138.
180 J. Lee, J. S. Kim, S.-Y. Moon, C. Y. Park, J. F. Kim and Y. M. Lee, *J. Membr. Sci.*, 2020, **595**, 117535.
181 R. Swaidan, B. Ghanem and I. Pinnau, *ACS Macro Lett.*, 2015, **4**, 947–951.
182 H. W. H. Lai, F. M. Benedetti, J. M. Ahn, A. M. Robinson, Y. Wang, I. Pinnau, Z. P. Smith and Y. Xia, *Science*, 2022, **375**, 1390–1392.
183 Z. Tong and W. S. W. Ho, *Sep. Sci. Technol.*, 2017, **52**, 156–167.
184 Y. Han and W. S. W. Ho, *J. Polym. Sci.*, 2020, **58**, 2435–2449.
185 L. Xiong, S. Gu, K. O. Jensen and Y. S. Yan, *ChemSusChem*, 2014, **7**, 114–116.
186 P. Li, Z. Wang, Y. Liu, S. Zhao, J. Wang and S. Wang, *J. Membr. Sci.*, 2015, **476**, 243–255.
187 M. Saeed and L. Deng, *J. Membr. Sci.*, 2015, **494**, 196–204.
188 K. Yao, Z. Wang, J. Wang and S. Wang, *Chem. Commun.*, 2012, **48**, 1766–1768.
189 A. Klemm, Y.-Y. Lee, H. Mao and B. Gurkan, *Front. Chem.*, 2020, **8**, 637.
190 Y. Chen and W. S. W. Ho, *J. Membr. Sci.*, 2016, **514**, 376–384.
191 Y. Chen, L. Zhao, B. Wang, P. Dutta and W. S. W. Ho, *J. Membr. Sci.*, 2016, **497**, 21–28.
192 M. Z. U. Mustafa, H. B. Mukhtar, N. A. H. M. Nordin, H. A. Mannan, R. Nasir and N. Fazil, *Chem. Eng. Technol.*, 2019, **42**, 2580–2593.
193 M. Q. Seah, W. J. Lau, P. S. Goh, H.-H. Tseng, R. A. Wahab and A. F. Ismail, *Polymers*, 2020, **12**, 2817.
194 J. N. Krishnan, K. R. Venkatachalam, O. Ghosh, K. Jhaveri, A. Palakodeti and N. Nair, *Front. Chem.*, 2022, **10**, 781372.
195 D. L. Zhao, F. Feng, L. Shen, Z. Huang, Q. Zhao, H. Lin and T.-S. Chung, *Chem. Eng. J.*, 2023, **454**, 140447.
196 T.-S. Chung, L. Y. Jiang, Y. Li and S. Kulprathipanja, *Prog. Polym. Sci.*, 2007, **32**, 483–507.
197 J. Wu, C. Z. Liang, A. Naderi and T. S. Chung, *Adv. Mater.*, 2022, **34**, 2105156.
198 J. Wu and T. S. Chung, *Small Methods*, 2022, **6**, 2101288.
199 N. U. Kim, B. J. Park, M. S. Park, J. T. Park and J. H. Kim, *Chem. Eng. J.*, 2019, **360**, 1468–1476.
200 X. Jiang, K. Goh and R. Wang, *J. Membr. Sci.*, 2022, **658**, 120741.
201 H. Wu, X. Zhang, D. Xu, B. Li and Z. Jiang, *J. Membr. Sci.*, 2009, **337**, 61–69.
202 Y. Qin, P. Yeh, X. Hao and X. Cao, *Colloids Surf., B*, 2015, **127**, 247–255.
203 K. Friess, P. Izák, M. Kárászová, M. Pasichnyk, M. Laň, D. Nikolaeva, P. Luis and J. C. Jansen, *Membranes*, 2021, **11**, 97.
204 J. Guan, T. Huang, W. Liu, F. Feng, S. Japip, J. Li, J. Wu, X. Wang and S. Zhang, *Cell Rep. Phys. Sci.*, 2022, **3**, 100864.
205 Q. Xu and J. Jiang, *Mol. Syst. Des. Eng.*, 2022, **7**, 856–872.
206 J. W. Barnett, C. R. Bilchak, Y. Wang, B. C. Benicewicz, L. A. Murdock, T. Bereau and S. K. Kumar, *Sci. Adv.*, 2020, **6**, eaaz4301.
207 N. Peng, N. Widjojo, P. Sukitpaneenit, M. M. Teoh, G. G. Lipscomb, T.-S. Chunga and J.-Y. Lai, *Prog. Polym. Sci.*, 2012, **37**, 1401–1424.
208 J. M. Ponce-Ortega, M. M. Al-Thubaiti and M. M. El-Halwagi, *Chem. Eng. Process.*, 2012, **53**, 63–75.
209 I. U. Khana, M. H. D. Othman, A. F. Ismail, T. Matsuura, H. Hashim, N. A. H. M. Nordin, M. A. Rahman, J. Jaafar and A. Jilani, *J. Nat. Gas Sci. Eng.*, 2018, **52**, 215–234.
210 M.-L. Liu, Z.-J. Fu and S.-P. Sun, in *Hollow Fiber Membranes: Fabrication and Applications*, ed. T.-S. Chung and Y. Feng, Elsevier, 2021, pp. 253–274.
211 X. He, A. Lindbråthen, T.-J. Kim and M.-B. Hägg, *Int. J. Greenhouse Gas Control*, 2017, **64**, 323–332.
212 S. Rothemund and I. Teasdale, *Chem. Soc. Rev.*, 2016, **45**, 5200–5215.
213 X. Jin, T. Foller, X. Wen, M. B. Ghasemian, F. Wang, M. Zhang, H. Bustamante, V. Sahajwalla, P. Kumar, H. Kim, G.-H. Lee, K. Kalantar-Zadeh and R. Joshi, *Adv. Mater.*, 2020, **32**, 1907580.
214 J. Yin, C. Zhang, Y. Yu, T. Hao, H. Wang, X. Ding and J. Meng, *J. Membr. Sci.*, 2020, **593**, 117405.
215 R. M. Teodoro, L. C. Tomé, D. Mantione, D. Mecerreyes and I. M. Marrucho, *J. Membr. Sci.*, 2018, **552**, 341–348.
216 P. Luis, T. V. Gerven and B. V. D. Bruggen, *Prog. Energy Combust. Sci.*, 2012, **38**, 419–448.
217 C. H. Lau, P. Li, F. Y. Li, T.-S. Chung and D. R. Paul, *Prog. Polym. Sci.*, 2013, **38**, 740–766.
218 S. R. Reijerkerk, M. Wessling and K. Nijmeijer, *J. Membr. Sci.*, 2011, **378**, 479–484.
219 Y. Zhao and W. S. W. Ho, *J. Membr. Sci.*, 2012, **415–416**, 132–138.
220 T. C. Merkel, M. Zhou and R. W. Baker, *J. Membr. Sci.*, 2012, **389**, 441–450.
221 C. Castel, R. Bounaceur and E. Favre, *Front. Chem.*, 2021, **3**, 668867.

